CHAPTER 1

INTRODUCTION

1.1 General

Portland Cement Concrete (PCC), commonly known as concrete, is a man-made material primarily manufactured from a mixture of Portland cement, fine and coarse aggregate as well as water. The word “Cement” is derived from the Latin “Caementum” which was used by the Romans to denote the rough stone or chips of marble from which a mortar was made. “Concrete” is derived from “Concretus” which signifies “growing together” (Addis, 1986). Steel Fibre Reinforced Concrete (SFRC) is defined as concrete manufactured by dispersing discontinuous discrete steel wires (fibres) into concrete.

The increasing demand for improved load-carrying capacity in roads (which is the result of road traffic becoming heavier) was first satisfied by strengthening the sub-base rather than by the use of a wearing course with a load-carrying capacity of its own. It was quite natural that the first concrete pavements were constructed of plain concrete. In the early days, deep sections were provided for concrete ground slabs. Increased knowledge and experience in this field had substantially improved the understanding of the behaviour of concrete and concrete pavements. Design methods have been refined and thinner slabs were found adequate to carry loads and load repetitions similar to those carried by the thicker slabs.

With the gradual growth in road traffic and increase in not only vehicle numbers but also magnitude of axle loads in recent decades, it was a natural development to make un-reinforced concrete pavement slabs thicker. It is a well-known fact that plain concrete is a material with a low tensile strength compared to its compressive strength. A concrete ground slab is normally designed using the flexural strength of plain concrete, which in normal reinforced concrete structures is completely disregarded. Obviously, more in-depth thought is needed to improve the load-carrying capacity of these concrete pavements. A natural step would appear to be the use of reinforcement for strengthening concrete slabs.

Improved understanding of the behaviour of concrete pavement structures under different loading and environmental conditions as well as advances in material engineering has led engineers to improve concrete specifications. Recently, considerable interest has been generated in the use of SFRC and other engineered concrete composites. The most significant influence of incorporating

steel fibres in concrete is to delay and control the tensile cracking of the composite material. This imparts certain favourable properties to the concrete such as post-cracking strength and resistance to fatigue. The improved engineering properties of SFRC make it a viable material for concrete applications such as pavements. It is therefore not surprising that there have been phenomenal developments and advances in the use of SFRC during the last three decades.

SFRC pavements were found to provide superior performance compared to plain concrete as it allows reduction in the slab thickness and yet provide equivalent performance (Elsaigh et al., 2005). The use of steel fibres in concrete enables designers to increase joint spacing (Parker and Rice, 1977). Economics can be achieved not only with respect to the joint construction cost but also by reducing the number of positions where distresses are likely to occur. Performance of previous SFRC pavements also revealed that the use of steel fibres results in longer maintenance free intervals compared to plain concrete, thus less interruption to traffic (Vandewalle, 1990). The initial cost of SFRC pavements will be less than the cost of plain concrete only if the cost of the steel fibres can be offset by a reduction in the cost of supplying and placing the smaller concrete volume. However, from an economic point of view life cycle cost should justify the use of SFRC in road pavements.

SFRC pavements were found to provide equivalent performance compared to conventionally reinforced concrete pavements when equivalent amounts of reinforcement is used (Bischoff et al., 2003). However, the SFRC is found to reduce construction time, as the steel fibres are added directly as one of the concrete mix constituents, and no steel fixing or adjustment is required (Association of Concrete Industrial Flooring Contractors, 1999). The adjustment of the steel mesh is of particular concern, as it needs proper seating and care while placing and compacting the concrete. The reduced construction time can result in early opening to traffic. In addition, saving may also be made when considering the cost of the overlapping steel for the conventionally reinforced concrete pavements. The steel fibres provide multi-directional reinforcement throughout the thickness of the slab. The multidirectional reinforcement is useful for concrete pavements as it not only prevents the breaking off at edges where conventional reinforcement is not present (Grondziel, 1989) but also results in a slab section that is reinforced against both hogging and sagging actions.

Despite the increased demand for higher load-carrying capacity and improved pavement behaviour, the subject of ground slabs is not researched to the same extent as other structural elements. Failures of ground slabs are too common and can have serious implications with respect to road user cost and the general economy. Although the benefits of SFRC in pavements are reasonably know, the analysis of SFRC pavements is less established. The use of SFRC in pavements has been

slowed down by the absence of a reliable theoretical method that can be used to design these pavements. The research conducted here is aimed at promoting the use of SFRC in road pavements by providing supporting research to convince road authorities of the benefits in using SFRC.

1.2 Problem statement

Numerical models for the analysis of SFRC ground slabs are scarce. Numerical models developed to analyse plain concrete ground slabs cannot be applied to SFRC. Formulae based on elastic analysis, such as Westergaard (1926), ignore the post-cracking strength contribution of the SFRC to both the flexural strength and ductility of the slab. In fact, steel fibres mainly become active after cracking of the concrete matrix, which means that the un-cracked analysis is not appropriate. Modern design philosophies have abandoned “permissible stress” concepts in favour of utilising the actual reserve strength of materials and members.

To determine the ultimate load-carrying capacity in many instances, it is necessary to proceed beyond the initial cracking load and to evaluate the post-cracking strength reserve. Design formulae based on the yield-line theory may provide an improved approximation of the ultimate load when compared to the elastic theory approach such as models developed by Meyerhof (1962), Losberg (1978), Rao and Singh (1986) and Silfwerbrand (2000). The yield-line analysis requires that the material behaviour is ideally plastic and the yield lines are correctly hypothesised. These aspects are crucial to the magnitude of the calculated load-carrying capacity using models based on yield-line theory. The absence of ideal plastic behaviour dictates that yield-line analysis should not be used to analyse elements made of SFRC that exhibits softening behaviour.

To effectively account for the non-linear material behaviour of SFRC in the analysis of concrete pavements, non-linear finite element analysis is required. Finite element methods are increasingly used to analyse various types of structures and it can be employed to analyse SFRC pavements. More realistic results for the stresses and displacements of the ground slab can be obtained including the load-displacement (P-Δ) response. However, the success of a finite element analysis largely depends on how accurately the material behaviour, cracking behaviour, geometry, and boundary conditions of the actual boundary problem are defined.

Several material models have been proposed to determine the tensile stress-strain (σ-ε) relationship for SFRC due to the complexities associated with testing concrete in direct tension and measuring the stresses and strains. In the past, two approaches have been used to determine the tensile σ-ε relationship for SFRC. In the first approach, the laws of mixture are used in combination with

results from fibre pullout strength and direct tensile tests to predict the tensile σ-ε relationship (Lim et al., 1987 a, Lok and Xiao, 1998). In the second approach, the tensile σ-ε relationship is empirically determined using results from a deformation-controlled beam-bending test (Vandewalle, 2003). However, the availability of steel fibres with a variety of physical and mechanical properties, as well as various fibre contents being used, tends to complicate prediction of the tensile σ-ε relationship of the SFRC using these approaches.

In recent years, the tensile σ-ε relationships have been determined by inverse analysis (back-calculation) using flexural responses obtained from beam-bending test (Elsaigh et al., 2004, Alena et al., 2004 and Østergaard and Olesen, 2005). The advantage of these methods is that the flexural response of the SFRC can be obtained with minimal complexities compared to procedures requiring results from direct tensile tests. The disadvantage is that these methods are numerically demanding. However, the numerical solution capabilities of available computer programmes can be utilised to readily perform the analysis.

1.3 Research objectives and limitations

The primary objectives of this research are:

(1) To develop a generalised analytical method that can be used to determine the tensile σ-ε relationship for SFRC using experimental moment-curvature (M-ϕ) or load-deflection (P-δ) results from beams.

(2) To propose a new method for analysing SFRC pavements, since existing methods are inadequate. The proposed method utilises non-linear finite element technique to analyse ground slabs subject to static mechanical loading. Thus provision can be made to include the post-cracking strength of SFRC. The Loads due to change in weather conditions are beyond the scope of this study.

(3) To determine the effect of steel fibre content, concrete strength, support stiffness and slab thickness on the P-Δ behaviour of SFRC pavements.

1.4 Brief description of work

The work reported in this research includes results of both experimental and computational modelling of SFRC beams and ground slabs. Experimental results obtained by the author in previous studies are utilised as input for the developed computational modelling. The experimental work included a full-scale slab test. The SFRC slab contained 15 kg/m^3 steel fibres and was supported by a foamed concrete slab cast on a relatively thick concrete floor. A plate-bearing test

was performed on the surface of the foamed concrete prior to casting of the SFRC slab. Deformation-controlled beam-bending tests were conducted for SFRC beams manufactured using concrete from the same batch used for the slabs. Cube and cylinder tests were also carried out to determine the compressive strength and the Young's modulus for the SFRC concrete. Experimental studies conducted by other researchers were also utilised.

In the computational modelling, an inverse analysis method is developed to back-calculate the tensile σ-ε relationship for SFRC. Non-linear finite element analyses are conducted on SFRC beams and ground slabs whose material constitutive relationship is determined using the inverse analysis. The results from the finite element analysis are compared to experimental result to verify both the material and the finite element models. The combined approach of inverse analysis and non-linear finite element modelling is further used to analyse SFRC beams and ground slabs reported in other studies. Thereafter, the adjusted non-linear finite element model is utilised to theoretically study the behaviour of SFRC ground slabs with respect to change in steel fibre content, concrete matrix strength, support stiffness and the slab thickness.

Mathcad (2001), programming software with numerical solution capabilities, is used to perform the calculations for the inverse analysis method. MSC.Marc (2003), general finite element computer programme with capabilities to analyse low-tension materials, is used to perform the non-linear finite element analysis.

1.5 Research structure

The study is structured as follows:
Chapter 1: Includes general introductory information and the motivation behind the use of SFRC in pavements. The research problem and objectives as well as a brief description of the conducted work are presented.

Chapter 2: Includes discussions on SFRC introducing the strengthening mechanisms provided by the steel fibres and its effect in improving the mechanical properties of concrete. An overview is presented for the main crack concepts used in numerical analysis. The overview includes the discrete crack concept and elaborates on the smeared crack concept. Behavioural aspects of SFRC beams and slabs are discussed including SFRC ground slabs and beams as well as the assessment of post-cracking strength of SFRC. Existing constitutive material laws for SFRC are presented and critically discussed. Yield surfaces that consider the biaxial stress states of combined tension and compression is presented and discussed with respect to SFRC. Appropriateness of existing models used to analyse SFRC ground slabs is discussed including methods based on elasticity theory,

yield-line analysis and non-linear finite element. A short introduction is provided for the most popular support models. An elaborated critique is presented for existing non-linear finite element models proposed for the analysis of SFRC ground slabs. The critique mainly includes the type of finite element used, the material constitutive law, support model and the comparison between experimental and calculated P-Δ responses. Finally a summary and remarks are given.

Chapter 3: Contains the description of the experimental procedures and test results for SFRC slab, beams, cubes and cylinders as well as the plate-bearing test conducted on the surface of foamed concrete.

Chapter 4: Includes the description of the generalised analysis method used to calculate the tensile σ-ε relationship for SFRC. The method utilises the measured flexural response from beam-bending test to indirectly determine the tensile σ-ε relationship of SFRC. The method is implemented and evaluated by comparing calculated and measured tensile σ-ε, M-ϕ and P-δ responses for SFRC reported in the studies conducted by Lim et al. (1987 a and b). It also includes results of a parameter study conducted using hypothetical SFRC beams. The results of the parameter study serve as an aid to adjust the tensile σ-ε relationship that would be initially assumed.

Chapter 5: Contains a brief description of the MSC.Marc programme. The analysis method described in chapter 4 is used to determine the tensile σ-ε response for SFRC containing 15 kg/m^3 of steel fibres using the P-δ response of SFRC beams. The calculated material model is used in non-linear finite element analysis to analyse a hypothetical single element subjected to direct tension. Thereafter, the SFRC beam is idealised using shell elements. The correlation between the measured and calculated P-δ responses is discussed.

Chapter 6: This chapter starts with modelling the plate-bearing test conducted on the surface of the foamed concrete slab. The constitutive σ-ε relationship for the foamed concrete is back calculated using finite element analyses. Trial-and-error procedure was followed by changing the parameters on the compressive σ-ε relationship for the foamed concrete until reasonable match was obtained between the measured and calculated P-Δ responses. The constitutive relationship for the SFRC beam, determined in chapter 5, is used in conjunction with the adjusted support model for the foamed concrete to analyse the SFRC ground slab. Correlation between the calculated and measured behaviour are discussed. The SFRC ground slabs tested by Falkner and Teutsch (1993) are analysed to further appraise the computational modelling methods presented in this research.

Chapter 7: Includes the results of parameter analysis conducted for SFRC ground slabs. Hypothetical SFRC slabs are used in the analysis. The support layers are made of a wide range of typical support materials used in road pavements. The adjusted finite element model for the SFRC ground slab is used to determine the effect of the strength of concrete matrix, support stiffness, steel fibre content and the thickness of the SFRC slab.

Chapter 8: Contains the conclusions and recommendations.

Chapter 9: Contains the list of references.

Appendix A: Includes design values for hooked-end steel fibres and calculation of the load-carrying capacity of SFRC ground slab using Meyerhof formula.

Appendix B: Includes the Mathcad work sheets showing the calculated tensile σ-ε response for the SFRC beam tested by Lim et al. (1987 b).

Appendix C: Includes the Mathcad work sheets showing the results of the first estimate and the adopted tensile σ-ε response for SFRC beam containing 15 kg/m^3 of steel fibres. It also includes the subroutine used to expand the cracking model of MSC.Marc to allow the input for bilinear tensile softening behaviour.

Appendix D: Includes the Mathcad work sheets showing the calculated tensile σ-ε response for the SFRC used in slabs P3 and P4 tested and reported by Falkner and Teutsch (1993).

CHAPTER 2

LITERATURE REVIEW

2.1 Introduction

Steel Fibre Reinforced Concrete (SFRC) is a composite material consisting of a concrete matrix containing a random dispersion of steel fibres. The performance of some of the early SFRC pavements was found not to demonstrate a marked performance improvement or any other overall advantage when compared to conventional paving materials (Schrader, 1985). An evaluation study conducted for some of these pavements concluded that the problems were limited to overestimation of the effect of steel fibres (Packard and Ray, 1984). In contrast, some other SFRC pavements were found to yield a convincing performance (Johnston, 1984). In recent years, advancement in the physical and mechanical properties of steel fibres in addition to extensive laboratory studies on SFRC led to the use of steel fibres in various pavement applications.

Field investigations have shown that SFRC has much greater spalling endurance compared to plain concrete (Lankard and Newell, 1984). It was stated that cracks and joints of SFRC pavements do not spall as much as they do in plain concrete even when loaded well beyond what would be considered failure loads (Parker and Rice, 1977). An airfield survey conducted by Grondziel (1989) showed that the use of SFRC reduced corner and edge break-off. This was attributed to the improved shearing capacity of the SFRC. Elsaigh et al. (2005) conducted a full-scale experiment to evaluate the use of SFRC for road pavements and compare its performance to plain concrete under in-service traffic loading. The performance of thinner SFRC ground slabs was found comparable to thicker plain concrete slabs.

A comparison between SFRC and plain concrete will show that SFRC exhibits superior properties, such as notable improvements in both flexural strength and post-cracking strength. Ground slabs are structural applications that could benefit from these advantageous features. The design of these slabs is often based on an elastic analysis assuming un-cracked concrete. Using such a method for SFRC would ignore the post-cracking contribution the SFRC can make to both the flexural strength and post-cracking strength of the SFCR slab. However, the effect of the post-cracking strength can be accounted for by using analysis methods based on yield line theory. The use of these methods was found to underestimate the load-carrying capacity of SFRC ground slabs.

To effectively account for the behaviour of SFRC in the analysis of SFRC ground slabs requires a method, for instance non-linear finite element methods using appropriate material and support

models. Many attempts to develop a tensile and compressive stress-strain (σ-ε) response for SFRC were found in the literature. SFRC has a complex behaviour involving phenomena like cracking of concrete and interactive effects between concrete and steel fibres. These special properties of SFRC must be considered for all stages of the modelling and the computational process.

This chapter contains discussions on the behavioural and analytical aspects of SFRC with emphasis on ground slabs. The main components of non-linear finite element analysis of SFRC slabs including, constitutive material relations, representation of concrete cracking and support models for ground slabs are also discussed. Reviews of previous finite element studies on SFRC ground slabs are presented.

2.2 Why use steel fibre reinforced concrete?

There are several types of steel fibres that have been used in the past. Apart from other mix constituents, there are four important steel fibre parameters found to affect the properties of the composite, namely: type and shape, content, aspect ratio (the length divided by the diameter of steel fibre) and orientation of fibres in the matrix. Early steel fibres were cut from drawn wire or mill-cut, but these tend to de-bond from the concrete matrix when applying load to the composite. Recently, efforts have been made to optimise these parameters to improve the fibre-matrix bond characteristics and to enhance fibre dispersability (Soroushian and Bayasi, 1991). It was found that SFRC containing hooked-end stainless steel wires has superior physical properties to straight fibres. This was attributed to the improved anchorage provided and higher effective aspect ratio than that for the equivalent length of straight fibre (Ramakrishnan, 1985).

Laboratory-scale tests conducted by many agencies and researchers indicate that the addition of steel fibres to concrete significantly increases the total energy absorbed prior to complete separation of the specimen (Johnston, 1985). The presence of steel fibres was also found to improve fatigue properties (Johnston and Zemp, 1991), impact strength (Morgan and Mowat, 1984, Banthia et al., 1995) and shear strength (Jindal, 1984, Minelli and Vecchio, 2006). The improvement of the mechanical properties of SFRC is attributed to the crack controlling mechanism. Bekaert (1999) suggested that two mechanisms play a role in reducing the intensity of stress in the vicinity of a crack. These mechanisms are:

(1) Steel fibres near the crack tip resist higher loads because of their higher Young's modulus compared to the surrounding concrete. Refer to Figure 2-1(a).
(2) Steel fibres bridge the crack and transmit some of the load across the crack. Refer to Figure 2-1(b).

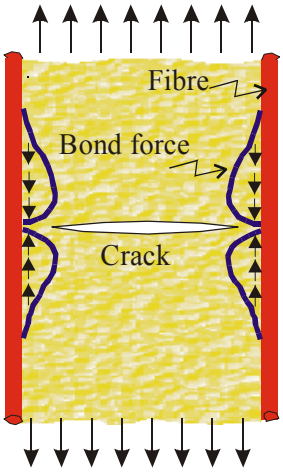

(a) Steel fibres at the tip of crack resist the crack growth (Parker, 1974).

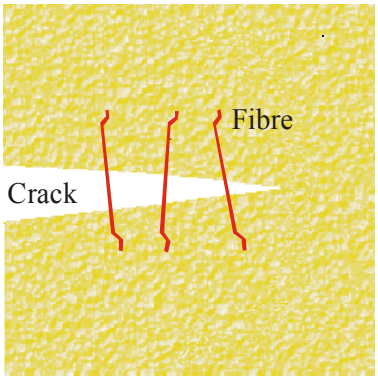

(b) Steel fibres across the crack transmit some tension (Bekaert, 1999).

Figure 2-1: Crack controlling mechanism provided by steel fibres.

The ability of the steel fibres to resist crack propagation is primarily dependent on the bond between the concrete and fibres as well as fibre distribution (spacing and orientation). The bond between the concrete and fibres is the mechanism whereby the stress is transferred from the concrete matrix to the steel fibres. The ability of the steel fibres to develop sufficient bond is dependent on many factors, mainly:

(1) The steel fibre characteristics (surface texture, end shape and yield strength).
(2) The orientation of the steel fibre relative to the force direction.
(3) The properties of the concrete.

In view of the significance of bond, attempts have been made to improve it, either by modification of the fibre characteristics or by matrix modification (Igarashi et al., 1996). It was suggested that if the deformed part of crimped steel fibres or the hooks of the hooked-end steel fibres act effectively, the fibre might fail by tensile yielding and rupture. In this case, it may appear that higher fibre yield strength is more advantageous. However, microscopic studies revealed that the higher steel fibre yield strength will result in more severe concrete matrix spalling around the steel fibre, thus limiting the further improvement in its reinforcement efficiency. It's therefore suggested that there is an optimal range of the steel fibre yield strength within which the best combination of peak pullout load and total energy absorption can be attained (Leung and Shapiro, 1999).

2.3 Failure of SFRC ground slabs

The behaviour of a centrally loaded SFRC slab is relatively linear up to the initial cracking at the bottom face of the slab where tensile stresses are the highest. The response then deviates slightly

from linearity after cracking and the slab continues to carry load until the cracks have extended to the edges and form a collapse mechanism. Substantial indentation occurs in the load introduction zone, whilst the corners of the slab are lifted up. The complete loss of load-carrying capacity occurs by punching shear (Bischoff et al., 2003). Based on the cracking progress, Falkner and Teutsch (1993) distinguished between three different behavioural regions. Referring to Figure 2-2, these three regions are:

(1) Region I: represents the initial un-cracked behaviour of the slab.
(2) Region II: is governed by the formation of small radial cracks in the central area where the load is applied.
(3) Region III: represents the behaviour when the cracks spread in the slab until collapse.

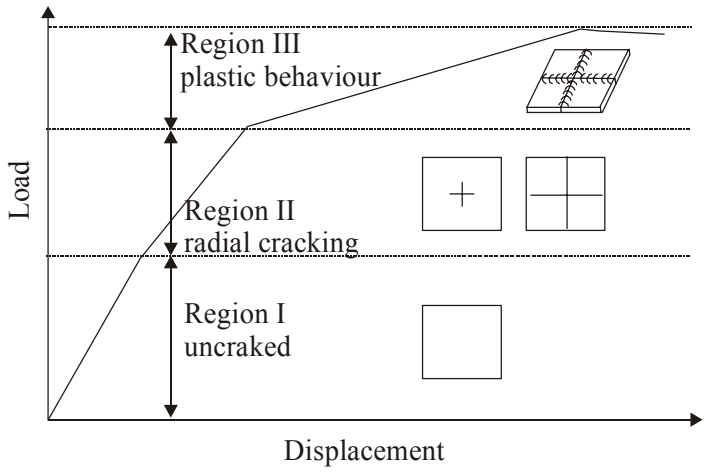

Figure 2-2: Typical load-displacement response of SFRC ground slab (Falkner and Teutsch, 1993).

Considerable energy is required for the crack to propagate to the surface and extend to the edges. It is therefore necessary to consider the post-cracking behaviour when designing SFRC ground slabs.

A distinction can be made between two different types of failure in concrete pavements. The first is a structural failure, which means that the pavement slab collapsed to the extent that the pavement is incapable of sustaining the loads imposed upon it. The second is a functional failure, which may or may not be accompanied by structural failure but is such that the pavement slabs will not carry out the intended function without causing discomfort or without causing high stresses in the vehicle that passes over it, due to roughness (Yoder and Witczak, 1975). Functional failure is often decided upon by using measurements related to the riding quality of the road. However, the functional failure of SFRC pavements is beyond the scope of this research.

Failure of ground slabs is typically based on serviceability issues, which deal with slab performance before cracking and the slab fails the serviceability criteria when it cracks. However, in service ground slabs often crack without total disruption of service. Coetzee and van der Walt, (1990) suggested that structural failure occurs when a slab is cracked and the crack has developed through the full depth along the sides of the slab. Falkner and Teutsch (1993) suggested that the decisions on failure of SFRC ground slabs are to be made based on the acceptable level of cracking. The load-carrying capacity of a SFRC ground slab can be determined based on the chosen crack level.

Generally, higher deflection values are associated with thinner slabs. Deflection must be considered when designing SFRC slabs because of the excessive deflections that might occur as a result of thinner SFRC sections. High deflections can lead to un-serviceable conditions that might be considered as functional failure of the pavement. In concrete road pavement design, the corner deflection is normally used as a worse case scenario for the deflection of concrete ground slabs. Corner loading was investigated by Beckett (1999) on two full-scale slabs measuring 5500 x 3000 x 150 mm and containing 20 kg/m^3 and 30 kg/m^3 of hooked-end steel fibre respectively. Apart from the increase of the corner load capacity due to the increase of steel fibre content, a reduction in vertical deflection value was found by increasing the steel fibre content (Beckett, 1999). These findings correlate well with the effect of the steel fibre content on the deflection of simply supported beam tested by Alsayed (1993).

2.4 Cracking models for concrete

The classical assumption about crack growth is that it is an essentially brittle process in which strength perpendicular to the crack drops to zero as soon as the crack has formed (Chen, 1982). For some materials this assumption is not fully correct as the tensile stress perpendicular to the crack does not drop to zero right away but decreases gradually (softens) as the crack opens. A major consequence of softening is that the material can neither be assumed to behave elastic-perfectly plastic nor elastic-perfectly brittle. Instead, the behaviour can be dealt with using the concept of elastic-softening formulation. Under the framework of finite element analysis of concrete structures, the cracking of concrete is primarily categorised into discrete and smeared approaches.

In the discrete crack approach, introduced by Ngo and Scordelis (1967), a crack is modelled as a geometrical discontinuity. The material behaves elastically until crack initiation, i.e. when maximum principal stress exceeds the limiting tension stress of the material. At a particular load beyond the cracking point the inter-element boundary nodes, where the limiting stress is exceeded, are released. Hence, the particular element is subject to the assumed tension softening

stress-displacement relationship σ (w). This procedure is repeated with every load increment until the energy (G_f) is exhausted in a process zone and eventually failure occurs. The fracture process zone is assumed to have a negligible thickness (hence the name discrete crack model). Fractured nodes affect the neighbouring elements, thus requiring modification of the element topology in the vicinity of the particular node. Several developments of discrete crack models exist. In general, simple discrete crack models use special interface elements, which must either be placed initially in predefined planes in the model in anticipation of cracks, or a re-meshing strategy is required for the elements in the vicinity of the crack.

In the smeared crack approach, introduced by Rashid (1968), a cracked solid is represented to be a continuum. In the earliest versions the effect of shear retention, Poison's ratio and tension softening were assumed to be negligible upon occurrence of crack initiation. In later versions, provisions were made to consider these effects. For instance, the effect of shear was considered as a percentage (shear retention factor) of the initial linear-elastic shear modulus (G). The representation of the tension softening behaviour of concrete in a " smeared" manner through a strain softening constitutive relation was first introduced by Bažant (1976) and further developed by Bažant and Oh (1983). Beyond the cracking point, the micro-cracks are smeared over a crack bandwidth and the material within this width is subject to the assumed tension softening stress-strain relation (σ-ε). Under increased loading the growth of this band is simulated by reducing the stiffness of the element/s (actually the stiffness at the Gauss points within it) that attains the prescribed fracture criterion in the direction normal to the direction of propagation. On the bases of extensive test data on plain concrete beams, Bažant and Oh (1983) recommended that the crack bandwidth is equal to three times the maximum aggregate size used in concrete. If a larger or smaller crack bandwidth is used, the softening σ(ε) relation must be adjusted in order to ensure that the energy dissipation is unaltered. In analysis involving the smeared crack approach, the element size can be set equal to the crack bandwidth. Therefore, the fracture energy should be released over this width in order to obtain results that are objective with regard to mesh refinement. Several researches have proposed different ways to relate the crack bandwidth to the size of finite element. To this end, the analysis method will only ensure objectivity if localisation indeed occurs in a single row of finite elements, for example: In the case of a beam in flexure, a single row or single column of elements; and in the case of a slab, a diagonal series of elements. If this is not the case, the fracture energy assigned to material points and scaled to finite element size leads to erroneous estimation of toughness.

The discrete crack approach is deemed to best fit the natural conception of fracture since it generally identifies fracture as a true geometrical discontinuity whereas a smeared representation is

deemed to be more realistic considering the "bands of micro-cracks" that form the blunt fracture in matrix-aggregate composites like concrete. The discrete crack approach implies a continuous change in nodal connectivity, which does not fit the nature of a finite element displacement method, as the crack has to follow a predefined path along element edges. The smeared crack approach is attractive because the original finite element mesh can be maintained and the orientation of the crack planes are not restricted, hence it is easier to implement in non-linear incremental analysis. However, it has generally been found to not only be somewhat less efficient numerically than a discrete crack model but also to be somewhat mesh sensitive (Karihaloo, 1995).

In many cases there is little to choose between the discrete and smeared approaches and the choice between them is a matter of convenience and might be limited only by the availability of a finite element program. In some cases the choice is based on the purpose of the analysis. For instance, if the overall P-δ response is desired, without regard for completely realistic crack patterns and local stresses, the smeared-crack model is probably the best choice. If detailed local behaviour is of interest, adaptations of the discrete-cracking model are useful (Chen, 1982). In some other cases the choice is based on the nature of the cracking pattern of the boundary problem under consideration. For instance, the smeared crack approach is more suitable for concrete structures with densely distributed reinforcement and / or with redundant supports that can assure formation of multiple cracks. To this end, the reinforcing action of the steel fibres in concrete affects the nature of the cracking of SFRC structural elements in a manner that diffused crack patterns tend to occur rather than discrete cracks. However, the final fracture is often dominated by a widening of a single crack. To some extent, this situation is conceived to provide a true physical basis for smeared crack concepts.

Smeared cracking concepts can be categorised into single-fixed, rotating and multiple fixed crack formulations. The fundamental difference between the three formulations lies in the orientation of the crack, which is either kept constant (single-fixed), or updated in a stepwise manner allowing secondary cracks to develop if a predefined threshold angle is exceeded (multiple fixed), or updated continuously (rotating). In the single-fixed smeared crack model, the orientation of the crack (i.e. the direction which is normal to the crack plane) coincides with the maximum principal stress orientation at crack initiation, and it remains fixed throughout the loading process. However, the principal stresses can change their orientation and can exceed the tensile strength of the concrete. In this case, the single-fixed smeared crack approach predicts a numerical response that is stiffer than the experimental observations (Rots, 1988). In a rotating crack model as introduced by Cope et al. (1980), the orientation of the crack plane is adjusted to remain orthogonal to the direction of the current major principal stress, where it is assumed that the axis of principal stress coincides with the axes of principal strain. The multiple fixed crack model, introduced by de Borst

and Nauta (1985), is an expansion of the fixed crack model in which the artificial stiffness of the fixed crack model is avoided by allowing for the formation of secondary cracks. Once they have been initiated, all existing cracks remain fixed in their initial orientation. The primary crack is initiated analogous to the fixed crack model. Secondary cracks are activated, when the change in principal stress direction, with regard to the previously activated crack, exceeds the threshold angle (α).

In the smeared crack approach, two methods are used to represent the strain following crack initiation. In one method the total strain is used while in the other method the strain is decomposed. The latter method does seem to have some benefits over total strain. In this method, the strain is decomposed into two components and the material is assumed to be no longer isotropic. Hence the total strain (ε), which is related to the displacement of the nodal points of a particular element, through the shape function, is divided into strain components describing the strain of the "uncracked material" or continuum (ε^{co}) and the so-called crack strain (ε^{cr}) by the relation as in Equation 2-1:

$$\varepsilon = \varepsilon^{co} + \varepsilon^{cr} \qquad (2\text{-}1)$$

Comparing the performance of the three crack models, Rots (1988) stated that the difference between single fixed, multiple fixed and rotating crack concepts and even the differences between smeared and discrete approaches vanish if the lines of the mesh can be adapted to the lines of the fracture in a boundary problem, which eliminates stress rotation beyond fracture. In the analysis conducted by Weihe et al. (1998) on a tension-shear boundary problem, for identical material parameters, the characteristic response differs significantly for three smeared crack models (refer to Figure 2-3). The differences are caused by the rotation inherent to the boundary problem and the fundamentally different assumptions inherent to these models. Figure 2-3 also shows that all smeared crack models provide an immediate relaxation of the principal stress as the primary crack is initiated. However, the fixed crack model exhibits a steady increase of the stress state as soon as the principal axes of stress rotates significantly from the primary crack. Eventually, the principal stress exceeds the critical stress limit. The rotating crack model shows a totally different behaviour. The softening response follows the microphysical prescribed exponential decay exactly. The response of the multiple fixed crack model is the same as the behaviour of the fixed crack model until a secondary crack orientation is activated.

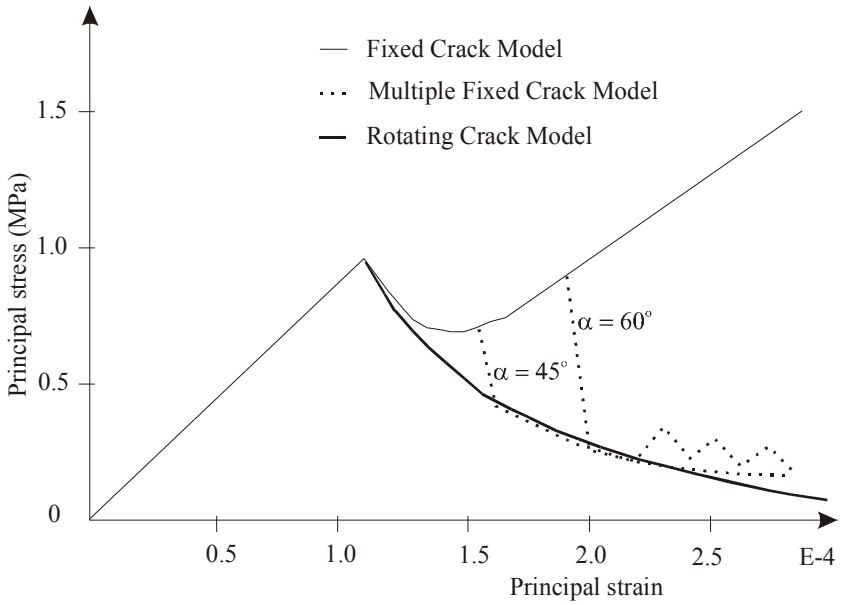

Figure 2-3: Response of smeared-crack models (Weihe et al., 1998).

During the post-cracking stage, the cracked SFRC can still transfer shear forces through aggregate interlock and /or due to the crack bridging action provided by the steel fibre reinforcement. Shear stresses are transmitted over the crack faces but with reduced shear capacity. To account for the effect of shear during the process of material degradation, the concept of a shear retention factor is often used to couple the shear behaviour to the degradation of the material. The shear retention factor relates the ratio of the post-cracking shear stiffness in the concrete to the pre-cracking shear stiffness. It essentially serves the purpose of ascribing some shear strength to the cracked concrete. In the literature a scatter of values ranging between zero and one were used. Hu and Schnobrich (1990) stated that the particular value chosen for the shear retention factor is not critical for mode I fracture but values greater than zero are necessary to prevent numerical instabilities. The mode I refers to planar symmetric state of stress which causes a crack to open, i.e. the crack faces are displaced normal to their plane, also referred to as opening mode. A constant value for the shear retention factor might not be appropriate as the shear stiffness reduces as loading is increased beyond the cracking point. Indeed, Swamy et al. (1987) relates the value of the shear transfer stiffness to the crack width as in Equation 2-2.

$$G_S = 2.5 \text{ x} \left(\frac{1}{w}\right)^{1.75} \qquad (2\text{-}2)$$

where G_S is the mean shear transfer stiffness in N/mm^3 and w is the crack width in mm.

2.5 Load-deflection behaviour of SFRC ground slabs

Extensive research has been conducted to investigate the influence of the steel fibres on the load carrying capacity of ground slabs (Kaushik et al., 1989, Beckett, 1990, Falkner and Teutsch, 1993, Bischoff et al., 1996, Elsaigh, 2001, Bischoff et al., 2003 and Chen, 2004). In these studies, full-scale slab tests were conducted to compare the behaviour of centrally loaded SFRC slabs to plain concrete or Welded Wire Fabric (WWF) reinforced concrete slabs. It was demonstrated that the addition of the steel fibres increase the load-carrying capacity of ground slabs significantly.

Figure 2-4(a) and (b) show the load-displacement (P-Δ) responses from two investigations conducted by Chen (2004) and Falkner and Teutsch (1993) respectively. It is prominent that SFRC containing hooked-end steel fibres yields greater load-carrying capacity compared to both plain concrete and SFRC containing mill-cut fibres (straight fibres having a relatively low tensile strength). Figure 2-4(a) shows that the addition of 30 kg/m^3 of hooked-end steel fibres resulted in greater load-carrying capacity for the SFRC ground slab compared to addition of 20 kg/m^3 of similar steel fibres type.

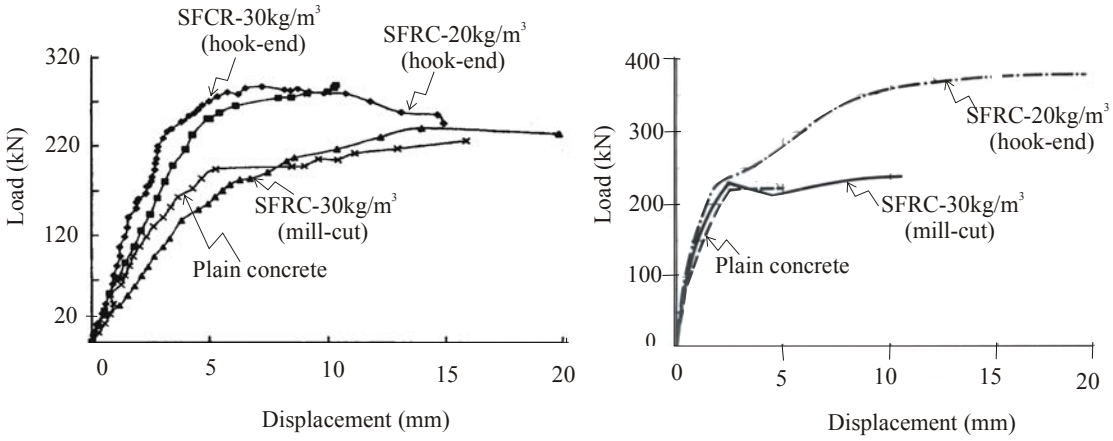

Figure 2-4: Comparison between SFRC and plain concrete ground slabs.

Bischoff et al. (2003) conducted full-scale slab tests to investigate the performance of WWF and SFRC. The slabs cast on either a loose or compacted subgrade with respective modulus of subgrade reaction of 0.015 MPa/mm and 0.75 MPa/mm. In one group of slabs, hook-end steel fibres were added to provide reinforcement at 0.16 percent (10 kg/m^3) and 0.38 percent (30 kg/m^3) by volume. In a second group of slabs, WWF were placed in both a single layer located 50 mm below the top face of the slab and double layers located 50 mm from top and bottom faces respectively. The size

of the WWF reinforcement was selected to provide 0.16 and 0.45 percent per volume for single layer and double layers respectively. These amounts of WWF reinforcement were selected on the basis of providing comparable post-cracking strength to the SFRC with respect to flexural beams.

Figure 2-5(a) shows the *P-Δ* response of SFRC and WWF reinforced concrete ground slabs on loose subgrade. When equivalent amounts of either WWF or steel fibre reinforcement are used, based on similar post-cracking strength values, the slabs exhibit comparable behaviour. For this reason, SFRC can be considered a suitable alternative to WWF reinforcement of concrete ground slabs. The difference in behaviour between the SFRC slab containing 0.38 percent by volume steel fibres and the slab with the double layer WWF reinforcement arise mainly because of the layer placed 50 mm above the bottom of the slab where it is more effective in resisting loading associated with positive moments. It is worth noting that the results from bending-beam tests containing double WWF layers (0.45 percent by volume) also showed greater post-cracking strength compared to that of SFRC containing 0.38 percent by volume.

Figure 2-5(b) shows the *P-Δ* responses of SFRC ground slabs on loose and compacted subgrade. The test results demonstrate the benefits of reinforcing concrete ground slabs using steel fibres to compensate for poor or loose subgrade. Although the benefit of using SFRC for ground slabs placed on poor subgrade is known, the amount of steel fibres needed to compensate for a particular poor subgrade is unknown. An analysis method is required to optimise the support stiffness and the steel fibre content for SFRC ground slabs to provide a desired load-carrying capacity.

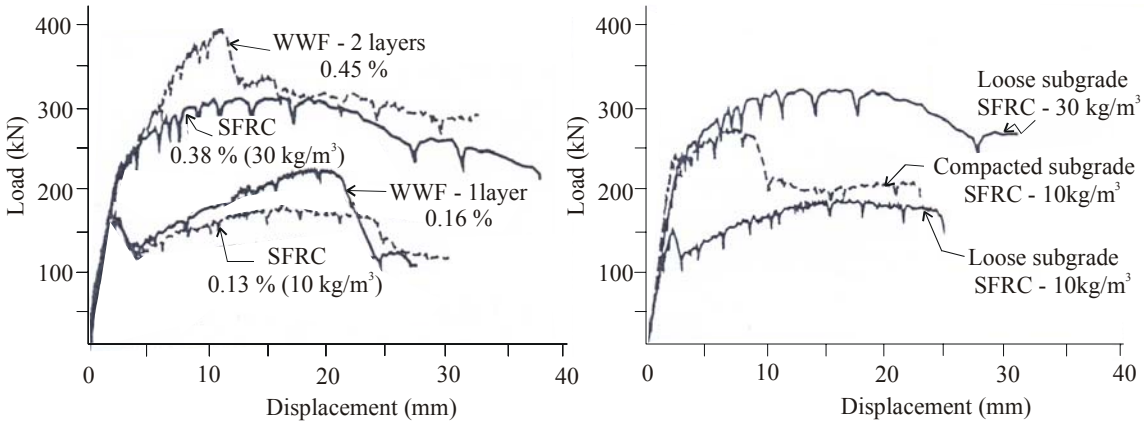

(a) Comparison between SFRC and WWF reinforced concrete ground slabs.

(b) Subgrade influence on SFRC slab response.

Figure 2-5: SFRC and WWF reinforced concrete ground slabs tested by Bischoff et al. (1996).

Several explanations for the increased carrying capacity of SFRC ground slabs have been suggested. Besides the structural ductility of the statically indeterminate slab, it has been recognised that the post-cracking strength of the steel fibre reinforced concrete is the reason behind the increased carrying capacity of SFRC ground slabs (Kearsley and Elsaigh, 2003). Partial stress redistribution can take place due to the statically indeterminate nature of the slab. The presence of membrane action, also known as "arching action", in a restrained slab further contributes to the resistance. Restraint develops either because the ends of the slab are held from lateral movement by the surrounding immovable concrete (Chen, 1982, Shentu et al., 1997) or due to friction between the slab and the supporting layers (Chen, 2004). The punching shear resistance can also play a significant role in increasing the bearing capacity of SFRC ground slabs. Experiments on slab-column connections, suggests that the introduction of steel fibres decreases the angle of the shear failure plane of the slabs which moves the failure surface away from the column face, hence resulting in an increase in punching shear resistance, and therefore an increase in the bearing capacity of the slab (Harajli et al., 1995).

The results from the static tests on the full-scale ground slabs presented in Figure 2-4 indicate that an appreciable thickness reduction, depending on steel fibre content, is possible for SFRC ground slabs when compared to counterpart plain concrete slabs. Indeed, it was found that about 16 percent thickness reduction is possible if 15 kg/m^3 of hooked-end steel fibres is used (Elsaigh, 2001). Bischoff et al. (2003) stated that the thickness reduction is justified by the following arguments:

(1) The addition of steel fibres significantly increases the flexural capacity and therefore the slab thickness can be reduced.
(2) The post-cracking strength of the SFRC allows for redistribution of stresses leading to an increased load-carrying capacity and therefore the slab thickness can be reduced.
(3) The use of steel fibres improves the fatigue resistance of the concrete, allowing for a smaller safety factor, which can lead to thinner slabs as the allowable stress is increased.

SFRC is deemed to be a superior material for concrete roads due to its improved mechanical properties compared to plain concrete. Although support provided by the subgrade means that bending stresses in pavements are generally low, the flexural capacity of the pavement remains an important aspect to consider. This is especially so when the bending stresses increase significantly due to uneven subgrade erosion, as is common in the case when the subgrade subsides at the pavement corner or edge. In conventional reinforced concrete pavements, the steel reinforcement is placed between the mid to two third depth to mainly resist stresses caused by changes in environmental conditions (Paramasivam et al., 1994). The load-carrying capacity of a concrete pavement can be enhanced by placing the reinforcement in the bottom of the slab. Thus allowing the concrete in the bottom surface to crack and the reinforcement there to take up the positive

moment. Top reinforcement can also be provided especially at corners and edges to resist negative moments (Losberg, 1961). SFRC and WWF reinforced concrete ground slabs were found to yield similar load-carrying capacities when equivalent amounts of reinforcement are provided (Bischoff et al., 2003). The steel fibres provide a slab cross-section that is reinforced against both hogging and sagging bending stresses. These stresses can arise in road pavements not only as a result of mechanical load but also as a result of curling and warping.

2.6 Flexural properties of SFRC

The flexural behaviour of SFRC is often studied using the load-deflection (P-δ) response derived from beam specimens tested under displacement control. The addition of steel fibres enhances the post-cracking strength of concrete. Figure 2-6 shows typical P-δ curves obtained for SFRC and plain concrete beams (150 x 150 x 750 mm), subject to third point loading. It can be seen that the plain concrete fails in a brittle manner while SFRC could withstand some load in the post-peak stage. It can also be seen that the increase in the steel fibre content increases the magnitude of the post-cracking strength (Elsaigh and Kearsley, 2002).

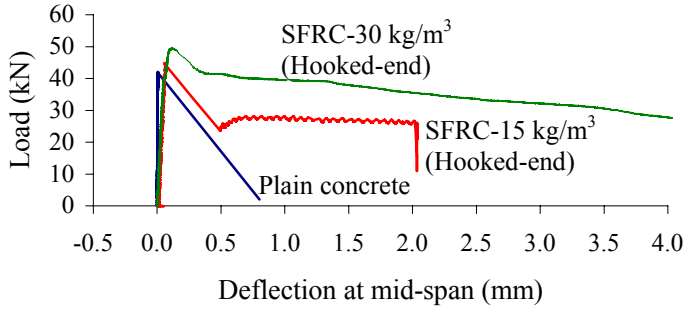

Figure 2-6: Load-deflection response (Elsaigh and Kearsley, 2002).

Although the magnitude of the flexural strength (calculated at the peak load) is increased when steel fibres are added to the concrete, this increase is not significant and is often not the reason for using steel fibres. This increase can also be attained through adjusting the concrete mixture design. Statically determinate structures, such as simply supported beams, do not explain the full advantage of using SFRC. When considering the P-δ responses of Figure 2-6 beyond the peak load, the beam cannot sustain this peak load for greater deflection values. Therefore, these beams would have failed at loads approximately equal to this peak load if load-controlled tests were performed rather than displacement-controlled tests. Full advantage of the post-cracking strength of SFRC can only be seen if plastic hinges and redistribution of stresses are taken into account in determining the load bearing capacity (Nemegeer, 1996).

Investigating the curve in Figure 2-6, one can distinguish between three behavioural stages:

(1) Ascending part of the curve up to the peak load.

(2) Descending part immediately beyond the peak load referred to as a region of instability. In this region unstable crack growth occurs, as the fracture energy does not match the elastic energy release, leading to a rapid increase in deformation. The occurrence of this deformation is faster than the response of the measuring devices (Chen et al., 1995). De-bonding, slipping and straining of steel fibres are assumed to take place in this stage.

(3) A third part in which the curve stays relatively flat at a load less than the maximum load.

The P-δ responses in Figure 2-7 are for two slabs measuring 1000 x 1000 x 50 mm and simply supported along their four edges. For the SFRC slab, the value of the peak load is reasonably sustained to a greater deflection compared to the plain concrete slab. The SFRC slab behaved in a ductile manner and sustained a peak load that is greater than the peak load sustained by the plain concrete slab. Both the structural ductility and the post-cracking strength of the statically indeterminate slabs were increased by the use of SFRC. Ductility at the structural level is achieved due to the fact that material failure occurs locally and in a gradual manner, thus allowing stress redistribution to take place.

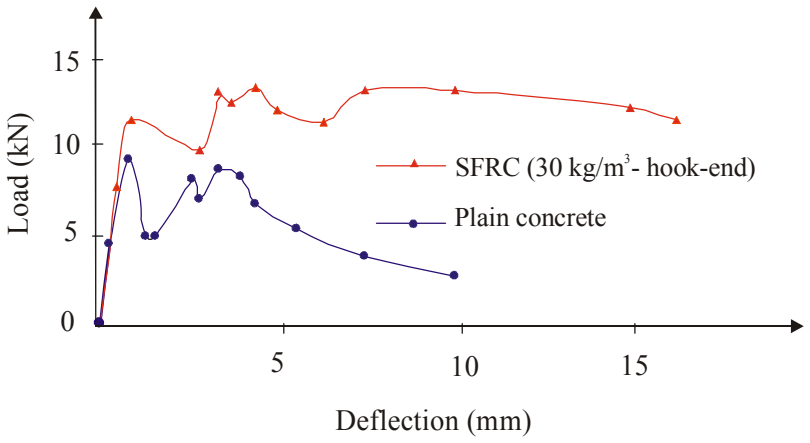

Figure 2-7: Load-deflection responses of slabs that are simply supported on their four edges (Sham and Burgoyne, 1986).

The area beneath the P-δ curve of a beam tested in displacement control is a measure of the energy required to achieve a certain deflection. This energy can be used to determine the post-cracking strength, which can be incorporated in design methods to estimate the load carrying capacity of SFRC members. The value of the post-cracking strength depends on the steel fibre type, steel fibre content and deflection limit. Although, the significant effect of steel fibres on concrete post-cracking

strength is widely recognised, there is uncertainty regarding a method to quantify it. The following three methods to interpret and calculate the ductility of SFRC are widely used:

(1) The ASTM C1018-97 method (1992) in which the energy absorbed up to a specified deflection is normalized by the energy up to the point of first cracking.

(2) The Japanese Concrete Institute method (1983), which interprets the post-cracking strength in absolute terms, as the energy required to deflect a beam to a mid-span deflection of 1/150 of its span.

(3) The RILEM TC 162-TDF Method (2002) has been developed recently. In this method, a notched beam subjected to a single load at mid span is used to generate the P-δ response.

In the method proposed by the Japanese Concrete Institute (1983) distinction should be made between several different terms viz, the flexural strength (f_{ct}), the equivalent flexural strength ($f_{e,3}$), the residual flexural strength ratio ($R_{e,3}$) and design flexural strength (f_d). The schematic P-δ response in Figure 2-8 is used to define and interpret these terms.

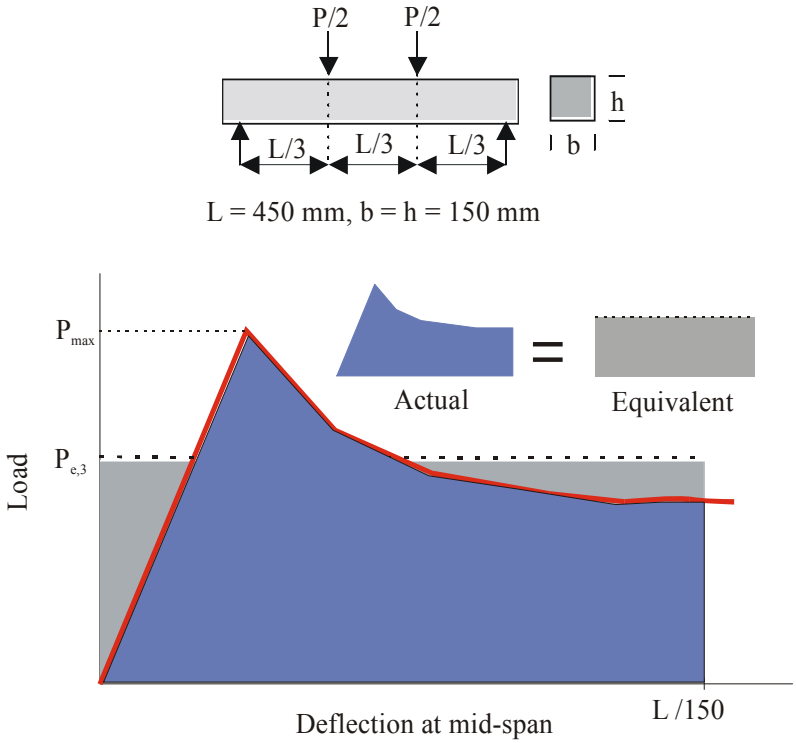

Figure 2-8: Schematic load-deflection curve for SFRC beam loaded at third-points.

The f_{ct} is the stress at peak load on the P-δ response. It can be calculated as in Equation 2-3:

$$f_{ct} = P_{max}\frac{L}{bh^2} \qquad (2\text{-}3)$$

where P_{max} = Peak load on the P-δ response.

L = Beam span.

h = Depth of the beam cross-section.

b = Width of the beam cross-section.

The $f_{e,3}$ is derived from the mean load corresponding to a deflection of L/150 in a third-point bending test and can be calculated as in Equation 2-4:

$$f_{e,3} = P_{e,3}\frac{L}{bh^2} \qquad (2\text{-}4)$$

where $P_{e,3}$ is the mean load calculated by dividing the area under the P-δ response by L/150.

The $R_{e,3}$ is the ratio between $f_{e,3}$ and f_{ct}. It represents the percentage of improvement of the flexural strength caused by addition of steel fibres. It can be estimated using the specification sheets provided by steel fibre manufacturer as in Table A-1 (refer to Appendix A) or it can be calculated if experimental results are available as in Equation 2-5:

$$R_{e,3} = \frac{f_{e,3}}{f_{ct}}100 \qquad (2\text{-}5)$$

The Meyerhof (1962) formulae can be used to explain the application of $R_{e,3}$ in designing the SFRC ground slabs. The strength term is modified to take the post-cracking strength of the SFRC into account (refer to the numerical example given in Appendix A). The Meyerhof formula for the interior load case is indicated in Equation 2-6:

$$P_i = 6.M_o.\left(1 + \frac{2r}{L_r}\right) \qquad (2\text{-}6)$$

where P_i = Interior load-carrying capacity of the slab.

M_o = Limit moment of resistance of the slab.

r = Radius of the loading plate.

L_r = Radius of the relative stiffness of the slab.

The radius of the relative stiffness is given as in Equation 2-7:

$$L_r = \left(\frac{E.d^3}{12.\left(1 - \mu^2\right)K} \right)^{0.25} \qquad (2\text{-}7)$$

where E = Young' modulus for the slab material.

d = Depth of the slab.

μ = Poisson's ratio of the slab material.

K = Modulus of subgrade reaction.

The limit moment of resistance for plain concrete is given as in Equation 2-8:

$$M_o = f_{ct}.\frac{b_o.d^2}{6} \qquad (2\text{-}8)$$

where b_o = a unit width of the slab.

The limit moment of resistance for SFRC is given as in Equation 2-9. The flexural strength term is modified to account for the post-cracking strength of the SFRC. The design flexural strength is determined as $f_d = (1+R_{e,3}/100)\, f_{ct}$ or the sum of $f_{e,3}$ and f_{ct}.

$$M_o = \left(1 + \frac{R_{e,3}}{100}\right) f_{ct}.\frac{b_o.d^2}{6} \qquad (2\text{-}9)$$

The relationship between the limit moment for plain concrete and SFRC can be useful. The thickness of a SFRC ground slab can be estimated if the adequate thickness of a plain concrete slab made from same parent concrete mixture is known. This can be achieved by comparing the load-carrying capacity of both slabs by using the Meyerhof formula. All inputs to this formula are approximately equal for both slabs except the flexural strength term and the thickness of the slabs. The term $\left[1 + 2r/L_r\right]$ in Equation 2-6 is also assumed to be the same for both slabs. The change in the value of this term due to the difference between the slabs thickness was found to be insignificant. The load-carrying capacity of plain concrete with a thickness of (d_p) and a flexural strength of (f_{ct}) can be calculated. The SFRC slab thickness (d_{sf}) that would take equal load to that of the plain concrete slab can then be calculated taking into account that the flexural strength term is equal to f_d.

For the plain concrete and the SFRC slabs to have equal load-carrying capacity, the moment terms in Equation 2-8 and 2-9 has to be equal.

$$f_{ct}\frac{d_p{}^2 \text{ x } b_o}{6} = \left(1+\frac{R_{e,3}}{100}\right) \text{x } f_{ct}\frac{d_{sf}{}^2 \text{ x } b_o}{6} \qquad (2\text{-}10)$$

By simplifying Equation 2-10, the thickness for the SFRC slab can be given as in Equation 2-11:

$$d_{sf} = \sqrt{\frac{(d_p)^2 \text{ x } 100}{(100+R_{e,3})}} \qquad (2\text{-}11)$$

Kearsley and Elsaigh (2003) experimentally verified the adequacy of this comparative design approach for ground slabs subject to static loading. Full-scale plain concrete and SFRC ground slabs were designed using this approach. Static loads were applied at the centre of the slabs. The measured P-δ responses show that the load-carrying capacity is approximately equal for both slabs.

Elsaigh et al. (2005) evaluated the validity of this comparative design approach with regard to traffic loading using results from a trial road subject to in-service traffic. A plain concrete section was designed to take approximately 60 x 10^3 E80s. This comparative design approach was used to design the SFRC slabs. The road section started to show some distresses after 400 x 10^3 E80s. The SFRC slabs were found comparable to the thicker plain concrete slabs.

2.7 Constitutive relationships for SFRC

The first pre-requisite for a successful finite element analysis is the definition of the constitutive behaviour of the material. Different techniques have been proposed to predict the tensile σ-ε response of SFRC. These techniques mainly include the laws of mixture and fracture energy.

2.7.1 Tensile stress-strain responses based on law of mixture and pullout strength

In these models, a volume-weighted sum of the concrete matrix and steel fibre responses are used to predict the composite behaviour in the pre-cracking stage while fibre pullout tests are used to predict the material behaviour in the post-cracking stage. The physical interaction between the concrete matrix and the steel fibres is usually accommodated through efficiency factors.

Lim et al. (1987a) developed a method to predict the pre-cracking and the post-cracking tensile behaviour of SFRC. The σ-ε response was modelled by considering the tensile behaviour of two identical SFRC specimens. The first set of specimens was un-cracked while the second set was pre-cracked. The parameters on the proposed σ-ε response were determined based on two different approaches. The law of mixture was used to predict the parameters for the pre-cracking stage while steel fibre pullout tests were used to determine the parameters of the post-cracking stage. In later work the σ-ε response was appraised by comparing measured and predicted P-δ responses for SFRC beams. The predicted P-δ responses, using the model, were found to match the measured responses (Lim et al., 1987b). The idealised tensile σ-ε response is shown in Figure 2-9(a). The notations in Figure 2-9 have been standardised to improve readability and eliminate confusion.

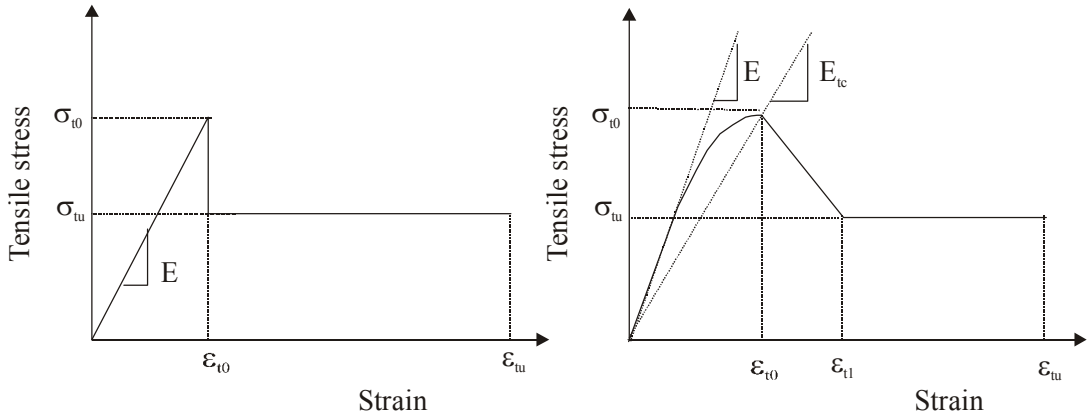

(a) Lim et al. (1987a)

(b) Lok and Xiao (1998)

Figure 2-9: Tensile stress-strain responses based on the law of mixture and steel fibre pullout strength.

The law of mixture is applied to define the pre-cracking stage as indicated in Equation 2-12 and Equation 2-13:

$$\sigma_{t0} = \sigma_m A_m + \sigma_f A_{eff} \qquad (2\text{-}12)$$

$$E = E_m V_m + E_f V_{eff} \qquad (2\text{-}13)$$

where σ_{t0} = Ultimate stress of the composite.

σ_m = Stress in the matrix.

σ_f = Stress in the steel fibre.

A_m = Area fraction of the matrix.

A_{eff} = Effective area fraction of the steel fibres.

V_m = Volume fraction of the matrix.

V_{eff} = Effective volume fraction of the steel fibre.

E = Young's modulus for of the composite (SFRC).

E_m = Young's modulus for the concrete matrix.

E_f = Young's modulus for the steel fibre.

Due to the random orientation of steel fibre in concrete, not all of fibres will be effective. However, only those fibres parallel or nearly parallel to the tensile stress are effective in controlling a particular crack. The amount of effective steel fibre is always of major concern when modelling SFRC structures and correction factors are often introduced to estimate the amount of effective steel fibres. The values for A_{eff} and V_{eff} equals the actual total areas and volumes of the steel fibres in the concrete multiplied by a selected factor.

The cracking strain of the SFRC (ε_{t0}) is often assumed to be equal to the failure strain of the concrete matrix (Pakotiprapha et al., 1983). However, experimental results revealed that the first-crack strain of SFRC is larger than the cracking strain of the matrix and it increases with increasing steel fibre content (Elsaigh and Kearsley, 2002). Based on the assumption that ε_{t0} increases linearly with the volume fraction of the steel fibre reinforcement, Nathan et al. (1977) developed an empirical expression to calculate ε_{t0} as shown in Equation 2-14:

$$\varepsilon_{t0} = V_{eff}\left(\varepsilon_{fp} - \varepsilon_m\right) + \varepsilon_m \qquad (2\text{-}14)$$

where ε_m is the cracking strain of the concrete matrix, ε_{fp} is the strain relating to the proportional limit of the steel fibres.

Equation 2-14 indicates that when the volume fraction of fibres is zero, ε_{t0} equals ε_m. Otherwise, ε_{t0} increases proportionately with increasing amount of fibres. The use of this expression does not imply that the steel fibres yield when the concrete matrix cracks.

In the cracked range, the behaviour is described by a combination of elastic deformation in the un-cracked sections and crack widening based on the bond-slip behaviour of the steel fibres at the crack. The ultimate tensile strength is related to the average ultimate pullout bond strength (τ_u) and

steel fibre length (L_f) as well as the steel fibre diameter (d_f). Referring to Figure 2-10, the stress in the cross-section of a single steel fibre (σ_{ui}) can be calculated as in Equation 2-15 where A_s and A_{fi} denote surface area and cross-section area of a single steel fibre respectively. The total stress corresponding to a certain effective volume of steel fibre (σ_{tu}) can therefore be calculated as indicated in Equation 2-16.

$$\sigma_{ui} = \tau_u \frac{A_s}{2A_{fi}} \qquad (2\text{-}15)$$

$$\sigma_{tu} = V_{eff} \tau_u \frac{L_f}{d_f} \qquad (2\text{-}16)$$

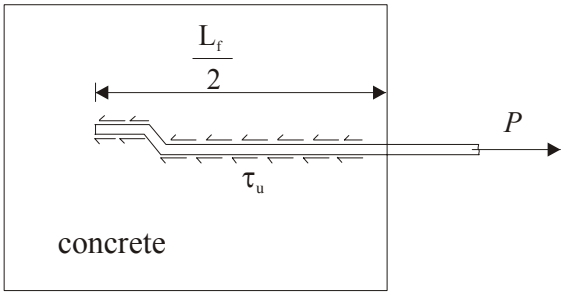

Figure 2-10: Finding the tensile stress for a single steel fibre from a fibre pullout test.

Table 2-1 shows values for the bond stress (τ_u) adapted from three different experimental studies. The variation in these results can be attributed to the different testing approaches followed by different researchers. In the tests conducted by Leung and Shapiro (1999) straight steel fibres were positioned to be inclined at 0, 30 and 60 degrees to the direction of the applied load. The embedded length of the steel fibre was kept constant in all tests. The pullout test carried out in this way was based on the fact that cracks in concrete member may intersect steel fibres at different angles. In the study by Shannag et al. (1997), the inclination angle was kept constant at zero degrees while the embedded lengths varied between 6, 12 and 18 mm. In the third study the angle of inclination and the depth were kept constant (Lim et al. 1987a). These tests were conducted using special specimens mainly made of cement-sand mortar that were prepared using different procedures than those applied in the production of the SFRC. In these three studies, the pullout-extension curve was established for the different specimens and the τ_u was calculated by dividing the maximum pullout load by the surface area of the embedded part of the steel fibre. This means that the assumption is

made that an average constant τ_u exists along the whole embedded length of the fibre. Conclusive recommendations for specifying τ_u can hardly be drawn from these results. The availability of a wide range of steel fibres and concrete matrix strengths contribute to an even greater uncertainty over bond stress values.

Table 2-1: Bond stress values adapted from existing research.

Study	Bond stress (τ_u) (MPa)
Leung and Shapiro (1999)	2.4 - 3.7
Shanag et al. (1997)	1.75 - 4.6
Lim et al. (1987b)	5.9 - 6.9

The area and the volume of the effective steel fibres can be calculated by applying correction factors to the actual volume of steel fibre added to the concrete mixture. Swamy and Al-Ta'an (1981) suggested the following corrections:

(1) Orientation correction factor (η_o). This is to account for the steel fibres, which are inefficiently oriented with respect to the principal tensile stress at particular sections.

(2) Length efficiency factor (η_l), defined as the ratio of the average steel fibre stress to maximum steel fibre stress. This is to account for the varying stress at the end portions of the steel fibre.

When steel fibres are uniformly dispersed in a large volume of concrete, they are expected to be randomly oriented with equal probabilities of being oriented in different directions. Correction must be made for those steel fibres that are ineffectively oriented in the volume space with respect to the direction of tensile stress. However, the proper correction to be used is uncertain. Romualdi and Mandel (1964) assumed an orientation correction factor equal to the ratio between average projected lengths of the steel fibres in one direction and the total length of these fibres.

In the study conducted by Soroushian and Lee (1990), the orientation factor was estimated by counting the effective steel fibres at fracture surfaces of nineteen SFRC beams. The beams, measuring 152 x 152 x 457 mm, contained various amounts of steel fibres and were subject to flexural loading. The steel fibres used were either straight or hooked-end with a length of 51 mm and a diameter of 0.5 mm. The results obtained from the measurements showed that the average η_o is equal to 0.62. However, different size as well as shape of specimen will certainly lead to a different value for η_o. It is also interesting to note that not only the shape of the cast volume

influences the orientation of steel fibres but also the compaction method has a significant effect on the manner that steel fibres align themselves. For example, steel fibres in concrete compacted by means of table vibration tend to align themselves in planes at right angle to the direction of the vibration (Edgington et al., 1974). The η_l is determined by Nathan et al. (1977) as in Equation 2-17 and Equation 2-18. These equations are incorporated in the material constitutive model developed by Lim et al. (1987a).

$$\eta_l = \begin{cases} 0.5 & \text{for } L_f < L_c \\ 1 - \dfrac{L_c}{L_f} & \text{for } L_f \geq L_c \end{cases} \qquad (2\text{-}17)$$

$$L_c = 0.5.\sigma_{fu} \frac{d_f}{\tau_u} \qquad (2\text{-}18)$$

where σ_{fu} is the ultimate fibre stress (fibre fracture stress) and L_c denotes the critical fibre length: defined as half the fibre length required to develop the ultimate fibre stress when it is embedded in the matrix.

Lok and Xiao (1998) proposed a three stage model to predict the tensile σ-ε response for SFRC. These three stages are the pre-cracking stage, immediately post-cracking stage and the post-cracking stage as indicated in Figure 2-9(b). It differs from the model of Lim et al. (1987a) in that a parabola was assumed for the first part of the σ-ε response and a middle stage was added. The pre-cracked stage is represented by the parabolic curve as in Equation 2-19:

$$\sigma = \sigma_{t0}\left[2\left(\frac{\varepsilon}{\varepsilon_{t0}}\right) - \left(\frac{\varepsilon}{\varepsilon_{t0}}\right)^2\right] \qquad (2\text{-}19)$$

where σ and ε denote the stress and the corresponding strain at any point on the parabolic curve. The ultimate tensile stress (σ_{t0}) is either measured from direct tensile tests or estimated by using Equation 2-12. The corresponding tensile strain ε_{t0} can be calculated using Equation 2-20. Based on the parabolic relationship in Equation 2-19, the value of E is determined as $2E_{tc}$. The value of σ_{tu} is calculated using Equation 2-16. In the third stage of the σ-ε response, the concrete matrix is assumed to be fully cracked with the steel fibres resisting all the tensile stresses. The value of ε_{t1} is

calculated using Equation 2-21. As far as the tension failure is concerned, Lok and Xiao (1998) suggested a value equal to 0.002 for the ultimate strain ε_{tu}.

$$\varepsilon_{t0} = \frac{\sigma_{t0}}{E_{tc}} \qquad (2\text{-}20)$$

$$\varepsilon_{t1} = \frac{\sigma_{tu}}{E_f} \qquad (2\text{-}21)$$

Some criticism has been levelled at the application of the "law of mixture concept" to predict the tensile strength of SFRC. The law of mixture requires that the fibre pullout resistance be mobilised to a large extent when the material reaches the peak stress. Soroushian and Bayasi (1987) suggested that bond slippages in the order of 0.38 mm need to take place before the pullout resistance of steel fibres in SFRC is mobilised. However, direct tension tests on SFRC indicate that the maximum crack openings at ultimate stress are in the order of 0.005 mm, which is far below the values needed for meaningful mobilization of the pullout resistance of steel fibres. This questions the use of the law of mixture concept to determine the ultimate tensile strength of SFRC, and it indicates that the pullout behaviour of fibres does not play a major role when the ultimate tensile stress of SFRC is reached. Models based on law of mixture were however claimed to provide satisfactory results when used to predict the response of SFRC beams (Lim et al., 1987 b).

2.7.2 Tensile stress-strain responses based on fracture energy

In these models the tensile σ-ε response for SFRC is developed using measured P-δ responses generated from a simply supported beam subject to a displacement-controlled bending test. The maximum tensile stress in the σ-ε response is determined as the stress with respect to the first crack load (when the P-δ response first deviates from linearity) on the P-δ response. The post-peak stresses and strains are calculated using the post-cracking strength based on the fracture energy of the tested beam. This modelling procedure adopts a macro approach rather than the micro approach adopted in the models presented in section 2.7.1.

Nemegeer (1996) proposed a tensile σ-ε response for SFRC by using a measured P-δ response generated from third-point beam testing. The shape of the σ-ε response and its defining parameters are shown in Figure 2-11(a). The ultimate tensile stress (σ_{t0}) is estimated as a percentage of the compressive strength. The ε_{t0} is then calculated assuming equal Young's modulus in tension and compression. The post cracking flexural strengths ($f_{ct,equ,150}$) and ($f_{ct,equ,300}$) at deflection values of

span length/150 and span length/300 respectively are calculated according to the method of the Japanese Concrete Institute (1983). The residual tensile stress after cracking and at the residual tensile stress at assumed failure are calculated as 37 percent of the respective post-cracking flexural strengths $f_{ct,equ,150}$ and $f_{ct,equ,300}$ respectively. The corresponding residual strain and failure strain are estimated as fixed values of 0.001and 0.01 respectively.

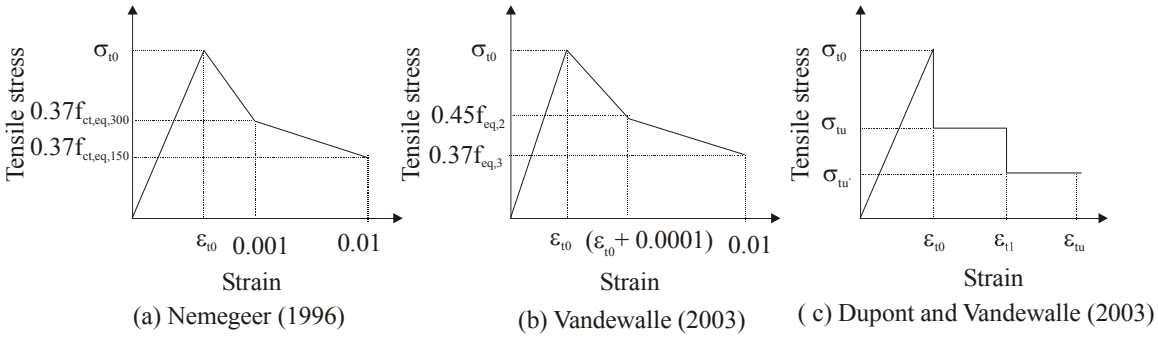

Figure 2-11: Tensile stress-strain responses based on the fracture energy.

Vandewalle (2003) has suggested a similar shape to the tensile σ-ε response presented in Figure 2-11(a) but the stress and stain parameters are estimated differently. The P-δ response is generated using a notched SFRC beam loaded at its mid span. The notched SFRC beam is cast and tested according to the method described in the RILEM TC 162-TDF (2002). The proposed response is shown in Figure 2-11(b). The ultimate tensile stress is calculated as the stress at initiation of cracking (when P-δ response first become non-linear) on the P-δ response. The load corresponding to initiation of cracking is determined as the highest load attained in the interval between 0 and 0.05 mm deflection in the measured P-δ response. The post cracking flexural strengths ($f_{eq.2}$) and ($f_{eq.3}$) at deflection values of 0.7 mm and 2.7 mm respectively are calculated according to the recommendation of the RILEM TC 162- TDF (2002). The residual tensile stress after cracking and at the residual tensile stress at assumed failure are calculated as 45 percent and 37 percent of the respective post-cracking flexural strengths $f_{eq.2}$ and $f_{eq.3}$ respectively. The ε_{t0} is then calculated assuming equal Young's modulus in tension and compression. The values of ε_{t1} and ε_{tu} are estimated as $\varepsilon_{t0} + 0.0001$ and 0.01 respectively. Yi-ning et al. (2002) stated that for steel fibre contents ranging between 20 and 60 kg/m^3, these strain values are satisfactory and relate to deflections of 0.7 mm and 2.7 mm in the P-δ response of the notched beam.

Dupont and Vandewalle (2003) suggested a two level shape for the post-cracking part of the σ-ε response (refer to Figure 2-11(c)). The pre-cracking stage of the response is established in a similar manner to that of the σ-ε response proposed in Figure 2-11(b). The post-cracking part of the curve

is established by assuming that ε_{t1} and ε_{tu} correspond to Crack Tip Opening Displacements (CTOD) of 0.5 mm and 3.5 mm respectively. Experimental tests have shown that a CTOD of 0.5 mm and 3.5 mm approximately correspond to strain values of 0.025 and 0.15 respectively. The corresponding stresses σ_{tu} and $\sigma_{tu`}$ can be calculated using static force and moment equilibrium for the cracked section of the beam by assuming specific values for the neutral axis depth.

In the σ-ε responses shown in Figure 2-11(a), (b) and (c), the tensile stress values at given strain limits were derived from P-δ responses. In these methods, the strains on the tensile σ-ε curve were empirically calculated based on the mid-span deflections of the beam specimen. The main concern is the accuracy and objectivity of calculating horizontal strains using vertical deflections (Kooiman et al., 2000). Tlemat et al. (2006) suggested that the main shortcoming of the RILEM tensile σ-ε response lies in the accuracy of the procedure adopted for the selection of the initial slope of the P-δ response. The procedure is subjective and therefore, it may not lead to the correct value of the load at initial crack on the P-δ response. In addition, the assumptions with respect to the depth of neutral axis are too simple to cater for the vast range of concretes with different matrix strength and steel fibre contents. It should be born in mind that the stress parameters of the σ-ε response are directly influenced by the values adopted for the load at initial crack and the neutral axis depths assumed for a particular strain.

2.7.3 Compressive stress-strain response

Adding amounts of steel fibres in the range of 10 to 60 kg/m^3 into concrete was found to have little or no effect on cube compressive strength and Young's modulus of the SFRC (Elsaigh and Kearsley, 2002). Previous work shows that the compression σ-ε responses proposed for plain concrete cannot adequately fit the post-peak response of SFRC (Ezeldin and Balaguru, 1992). In the analysis of SFRC beams the compressive σ-ε response for plain concrete, as recommended by BS 8110: 1985-Part 1, was used (Lok and Pei, 1998). Lok and Xiao (1999) recommend the use of the σ-ε responses developed for plain concrete but with some modification to ultimate compressive strain by using greater strain values for SFRC. Ezeldin and Balaguru (1992) proposed a uni-axial compressive σ-ε response as indicated in Equation 2-22. The proposed σ-ε response was later verified by experimental work conducted by Nataraja et al. (1999).

$$\frac{\sigma}{\sigma_{cu}} = \frac{\beta\left(\varepsilon/\varepsilon_0\right)}{\beta - 1 + \left(\varepsilon/\varepsilon_0\right)^{\beta}} \qquad (2\text{-}22)$$

where σ and ε = The stress and corresponding strain at any point in the curve.

σ_{cu} and ε_0 = Ultimate compressive strength and corresponding strain.

β = Material factor depending on the steel fibre type.

The material factor (β) for hooked-end steel fibres is estimated empirically from Equation 2-23:

$$\beta = 1.093 + 0.7132(\text{R.I.})^{-0.926} \qquad (2\text{-}23)$$

The reinforcing index (R.I.) for the hooked-end steel fibre relates to the weight fraction (w_f) and aspect ratio (L_f/d_f) of the steel fibres. The R.I. is calculated using Equation 2-24. The compressive σ-ε response can be established if R.I., σ_{cu} and ε_0 are known.

$$\text{R.I.} = w_f . \frac{L_f}{d_f} \qquad (2\text{-}24)$$

2.7.4 Yield surface

The σ-ε response for both tension and compression, discussed in the previous sections, were developed relying on a uniaxial stress state. The strength of concrete elements can be properly determined only by considering the interaction of various components of the state of stress. For example, Kotsovos and Pavlovic (1995) explained the importance of the interaction of stresses by using compressive test results of plain concrete cylinders under various levels of confining pressure. It was found that a small confining pressure, of approximately 10 percent of the uniaxial cylinder compressive strength, is sufficient to increase the load-carrying capacity of the tested cylinder by as much as 50 percent of the original value. On the other hand, a small lateral tensile stress of about 5 percent of the compressive strength of the cylinder is sufficient to reduce the load-carrying capacity of the cylinder by approximately the same amount.

In general, the failure of structural element can be divided into crushing and cracking types. Crushing indicates the complete rupture and disintegration of the material under compression. Cracking indicates a partial or complete collapse of the material across the plane of cracking under tensile stress states (Chen, 1982). The stress state in structures is often a combination of tension and compression.

Kupfer et al. (1969) conducted and experimental investigation to study the biaxial strength of concrete. In their experiment, prismatic concrete specimens measuring 200 x 200 x 50 mm were subjected to biaxial stress combinations in the regions of biaxial compression, compression-tension

and biaxial tension. Three types of concrete with unconfined compressive strength of 19, 31.5 and 59 MPa were tested at 28 days. Within each region of stress combinations four different stress ratios were chosen and six specimens were tested for each variable. Figure 2-12 shows the relationship between the principal stresses (σ_1 and σ_2) at failure given for the three types of concrete investigated.

Apart from the fact that the strength of concrete under biaxial compression is larger than under uniaxial compression, the relative strength increase is almost identical for the three types of concrete used. The large variation in the uniaxial strength of these three different concrete types has no significant effect on the biaxial strength. In the range of compression-tension, the compressive stress at failure decreases as the simultaneously acting tensile stress is increased. Under biaxial tension the controlling biaxial tensile stress is almost independent of the stress ratio and therefore the strength is almost the same as the uniaxial tensile strength. In other words, tension in one plane of concrete element does not affect the tensile properties of the perpendicular plane.

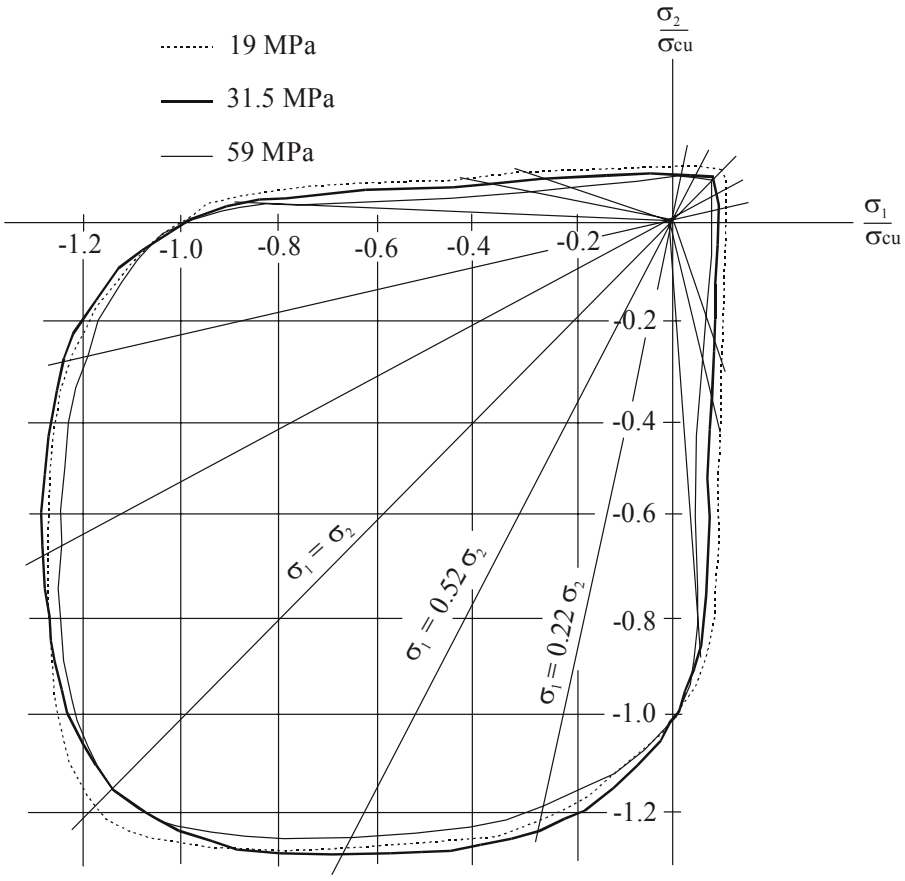

Figure 2-12: Biaxial strength of concrete - results of experimental investigation conducted by Kupfer et al. (1969).

Chern et al. (1992) investigated the influence of the presence of steel fibres on the behaviour of SFRC under multi-axial stress. In their investigation straight steel fibres with a length of 19 mm were used. The experimental results for plain concrete and SFRC cylinders are compared. The SFRC contains approximately 80 kg/m^3 of steel fibres (1 percent by volume). Figure 2-13 shows that the addition of steel fibres to concrete has an insignificant effect on the behaviour of the composite subjected to hydrostatic compression up to 70 MPa. It should be noted that this confining pressure was approximately three times the uniaxial compressive strength. It can be deduced that failure criteria, describing the compression behaviour under multiaxial stress state, that were successfully used for plain concrete are also appropriate for SFRC.

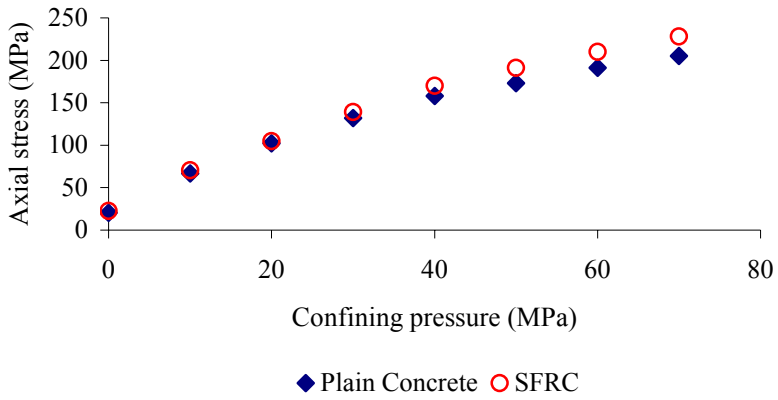

Figure 2-13: Comparison between behaviour of SFRC and plain concrete under compression multi-axial stress state.

In the finite element analysis of SFRC structures, various researchers have used different yield surfaces to describe the compressive regime. For example, Falkner et al. (1995b) used Von Mises and Hu et al. (2004) used the Mohr-Coulomb. The Von Mises yield surface can be described as a cylinder in the principal stress space σ_1, σ_2, and σ_3 (see Figure 2-14(a)). It assumes that yielding of a material begins when the maximum shearing stress at a point reaches a certain value and it is therefore insensitive to hydrostatic pressure. However, if yield is pressure-sensitive, the failure surface will not be a cylinder parallel to the hydrostatic axis as the cross-sections parallel to the deviatoric plane (plane perpendicular to hydrostatic axis) are different in size and need not be geometrically similar (Chen, 1982). The yield stress in concrete clearly depends on the hydrostatic pressure and therefore Mohr-Coulomb and Drucker-Prager yield criteria seem most suitable for concrete. The Drucker-Prager yield surface is a smooth approximation of Mohr-Coulomb (hexagonal shape in the deviatoric plane). It is a conical surface in the principal stress space for which all cross sections are assumed to be geometrically similar and the only effect of the pressure is to adjust the size of the cross sections in the various planes parallel to the deviatoric plane (see Figure 2-14(b)).

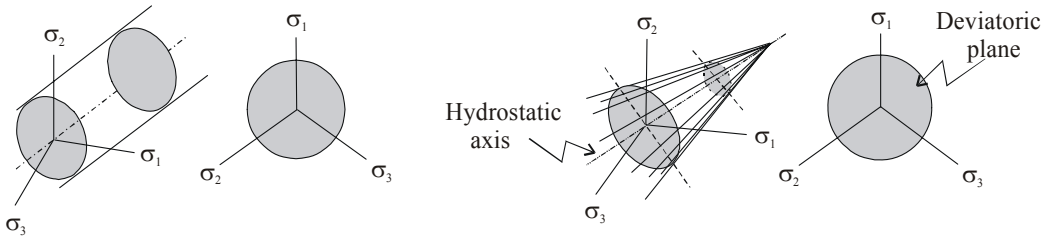

(a) Von Mises (b) Drucker-Prager

Figure 2-14: Yield surfaces for concrete.

Finite element analyses conducted in this research involve uniaxial response of beams and biaxial tension as well as biaxial compression stress states in slabs. These stress states can be modelled by combining crack detection surfaces and compression yield criterion to bound the tensile cracking and compressive yielding respectively. The maximum principal stress criterion of Rankine is widely used (see Figure 2-15(a)). According to this criterion, brittle fracture of concrete takes place when the maximum principal stress at a point inside the material reaches a value equal to the tensile strength of the material regardless of the normal or shearing stresses that occur on other planes through the point. This fracture surface is referred to as the fracture cut-off surface or tension-failure surface or simply tension cut-off (Chen, 1982). The yield of concrete can be described by a hydrostatic pressure dependent criterion such as Mohr-Coulomb or Drucker-Prager yield criteria. In the presence of compressive stresses in the region of compression-tension the cracking criterion must be adapted somewhat. Buyukozturk (1977) suggested that in a plane stress state the tensile strength is a linear function of the compressive stress as shown by the dashed lines in Figure 2-15(b).

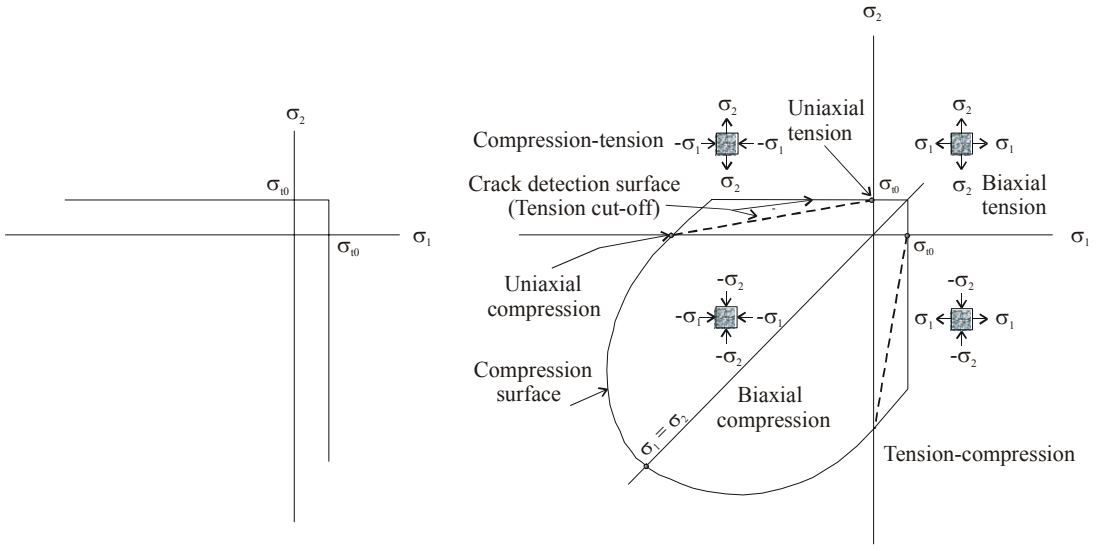

(a) Rankine (b) Rankine combined with Drucker-Prager

Figure 2-15: Combination of Rankine and Drucker-Prager.

2.8 Analysis of ground slabs

The thickness design of concrete ground slabs is the same as for other engineered structures where the aim is to find the optimum thickness that will result in minimal cost and adequate performance. In the assessment of SFRC ground slabs, ductility plays a decisive role in load-carrying capacity and deformation behaviour of these slabs. Existing analytical models for structural design of ground slabs can generally be divided into three categories:

(1) Methods based on elasticity theory, assuming an un-cracked structure.
(2) Methods based on yield line theory, assuming a cracked structure.
(3) Methods based on non-linear analysis. In these methods, the P-Δ response is computed from which the ultimate load can be determined.

Westergaard (1926) was the pioneer in developing analytical models for analysing plain concrete slabs supported on a Winkler foundation. Ioannides et al. (1985) conducted a study to re-examined Westergaard's equations. In their study, several empirical adjustments were considered and the slab size requirements for the development of infinite slab responses were established. The Westergaard model only enables us to determine when localised failure starts in perfect slabs, but it does not tell about the consequences of this localised failure. In other words no indication is given whether this leads to total failure or only to formation of harmless, small cracks (Henrik and Vinding, 1995). Methods based on elastic analysis (assumes concrete deforms linearly up to failure), can however hardly be applied to SFRC ground slabs, as they do not account for the post-cracking strength of the SFRC. In fact, steel fibres become active after cracking of the concrete matrix so that the un-cracked option is not appropriate for SFRC slabs.

Modern structural design codes of practice have abandoned "permissible stress" concepts in favour of utilising the actual capacity of materials and members. A design approach based on the yield line theory may provide an improved approximation of the load-carrying capacity of SFRC slabs compared to the elastic theory approach. Models developed by Meyerhof (1962), Losberg (1978) and Rao and Singh (1986) are based on yield line theory. These models were originally developed to estimate the load-carrying capacity for plain and conventionally reinforced concrete ground slabs. For these models to be used in designing SFRC, the strength term is changed and represented as the sum of the post-cracking strength and the cracking strength (refer to Appendix A). This modification will account for the stress redistribution as the result of incorporating steel fibres (Kearsley and Elsaigh, 2003). However, there are two basic prerequisites for the yield line theory to provide a good approximation for the ultimate load carried by concrete ground slabs. The first is that the material behaviour is ideally plastic to allow for bending moment redistribution (Holmgren, 1993). This is not the case with the SFRC often used for ordinary ground slabs (Meda and Plizzari,

2004). The second is that the yield lines are correctly hypothesized. This prerequisite is crucial because the magnitude of ultimate load is dependent on the pattern on the yield lines.

Falkner et al. (1995a) suggested a combination of the elastic theory and the yield line theory. They proposed some procedures for adjusting the Westergaard formulae to model SFRC ground slabs. In their proposed formula the load-carrying capacity is calculated by multiplying the load results obtained from the Westergaard formula with a factor to account for the effect of the post-cracking strength of the SFRC. These factors were determined from full-scale ground slab test results and finite element analyses.

Conflicting opinions exist regarding the applicability of the numerical models discussed here for SFRC ground slabs. Evaluation of these models is normally conducted by comparing measured results from full-scale slab test to calculated load-carrying capacity using these numerical models. It is often stated that certain models underestimate or accurately estimate the load-carrying capacity of the SFRC slab (Kaushik et al., 1989; Beckett, 1990, Falkner et al., 1995a and Chen, 2004). However researchers should be cautious when results from slab model tests are used to validate numerical models that can be used to design pavement slabs, which differ from the model slabs tested in the laboratory. The lack of edge restraint that is normally the case for slab models, allows the slabs to lift up from the supporting layers at the edges and corners. This is often not the case for pavement slabs as they are usually restrained by the next slab at joints (Bischoff et al., 2003).

If we are to seek a greater exploitation of SFRC, analysis should proceed beyond the initial cracking point. Recently, non-linear finite element methods were implemented to analyse SFRC ground slabs with different levels of success (Falkner et al. 1995b, Barros and Figueiras, 2001 and Meda and Plizzari, 2004). The advantage of using non-linear finite element methods is that the behavioural aspects can be obtained throughout the loading process. For example, the complete P-Δ response and associated stresses within the SFRC slabs can be obtained which is not achieved when using elastic theory or yield-line theory. Hence, an improved understanding of the behaviour of the SFRC structure, greater safety and improved economy can be achieved when utilising non-linear finite element methods. The accuracy of these methods is much dependent on the appropriateness of the material constitutive model and the representation of the cracks.

2.8.1 Models for support layers

The inherent complexity of soil characterisations has led to idealised models to describe the interaction between the soil and the slab. This complexity influences structural behaviour of concrete ground slabs. It is often essential to model the effect of a foundation on the structure

without taking details of stress or deformation in the foundation itself into account. Toward this end, various foundation models have been proposed and used in the analysis of ground slabs.

Winkler pioneered the modelling of subgrade in 1867 by introducing the concept of subgrade reaction. Westergaard (1926) expanded the concept in subsequent years to model the interaction of a rigid slab resting on soil foundation. The soil was modelled such that the force at a point of contact between the slab and the support is only dependent on the displacement at the same point. In other words, a certain pressure applied over a specific area causes uniform deformation over that specific area but there is no other deformation in the adjacent soil (refer to Figure 2-16). The standard method for obtaining the modulus of subgrade reaction in the field is prescribed in the ASTM- D 1195 (2004). The load-displacement relation is indicated in Equation 2-25:

$$\rho = K\Delta \qquad (2\text{-}25)$$

where K is the spring stiffness or modulus of subgrade reaction and Δ is the displacement under the area due to the pressure ρ.

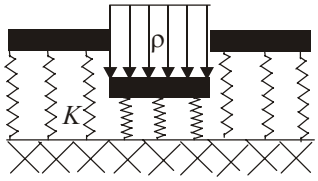

Figure 2-16: Schematisation of a concrete slab on a Winkler support model.

Another way of modelling the ground support is to use the semi-infinite continuum (half-space elastic model). The material model of the support is defined by Young's modulus and Poisson's ratio. The soil is modelled as an equivalent homogenous isotropic elastic layer of uniform thickness, underlain by a rough rigid base layer (Poulos and Small, 2000). Figure 2-17 shows the displacement profile due to the applied pressure. This support model allows the modelling of ground supports that includes different layers with different stiffness (MacLeod, 1990). This is not the case for Winkler's model as the overall effect of support is modelled. The Winkler model and the half-space elastic model provide significantly different responses when used to analyse a pavement system. This is because of the different assumption used in these two models. The actual behaviour of a ground support lies between the behaviours described by these two models (Zuhang, 1990 and Beckett, 2000).

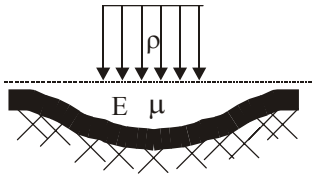

Figure 2-17: Schematisation of a concrete slab on half-space elastic support model.

Soil pressure measurements beneath full-scale tests on two concrete ground slabs, conducted by applying centre loading to the slab, have however shown that natural soil corresponds best to the linear elastic behaviour hypothesis (Losberg, 1961). In general the assumption of linear elastic behaviour of the soil-structure systems is assumed adequate and most appropriate for design purposes (Wood, 2000).

In finite element analysis of slabs and plates supported on ground, the Winkler support is extensively used (Cerioni and Mingardi, 1996, Shentu et al., 1997, Meda and Plizzari, 2004). Barros and Figueiras (2001) further recommended that a multi-linear or parabola soil pressure-displacement response be used instead of the linear response. Abbas et al. (2004) recommended the use of the half-space elastic support model that can be simulated by using three-dimensional finite elements. The shear deformation within the support and the usual singularities at the bottom of the slab directly under point loads applied at the top can thus be avoided.

2.8.2 Review of previous finite element models for SFRC ground slabs

Finite element analysis has been used by many researchers to analyse SFRC ground slabs. In this section, the non-linear finite element models developed by Falkner et al. (1995 b), Barros and Figueiras (2001) and Meda and Plizzari (2004) will be reviewed. In these three researches, the developed models were verified by comparing measured *P-Δ* responses to the response calculated using the particular model. Different finite element types, support models and material models were used.

2.8.2.1 Finite element model for SFRC ground slab developed by Falkner et al. (1995 b)

Falkner and Teutsch (1993) conducted a full-scale experiment on SFRC concrete ground slabs. In their experiment *P-Δ* responses were generated by testing SFRC slabs measuring 3000 x 3000 x 150 mm and containing 20 kg/m^3 of hooked-end steel fibres. The SFRC slabs were cast on a 60 mm thick support placed on a rigid floor slab. The support material was either cork or rubber with K-value equals to 0.025 and 0.05 MPa/mm respectively. The load was centrally

applied using a steel plate measuring 120 x 120 mm. A foil sheet was placed between the support and the slab to reduce the influence of shrinkage and expansion stresses on the SFRC slab.

Falkner et al. (1995b) developed a finite element model for SFRC ground slabs. The results from this experiment were used to verify the model. Due to symmetry, only a quarter of the slab was modelled. Eight-node isoparametric brick elements were used for the slab and the support (see Figure 2-18). However, the choice of single brick element over the thickness of the slab is not objective, as it cannot capture the stress profile. This is especially true when the load proceeds beyond the cracking point as a non-linear material is only represented at two integration points through the depth.

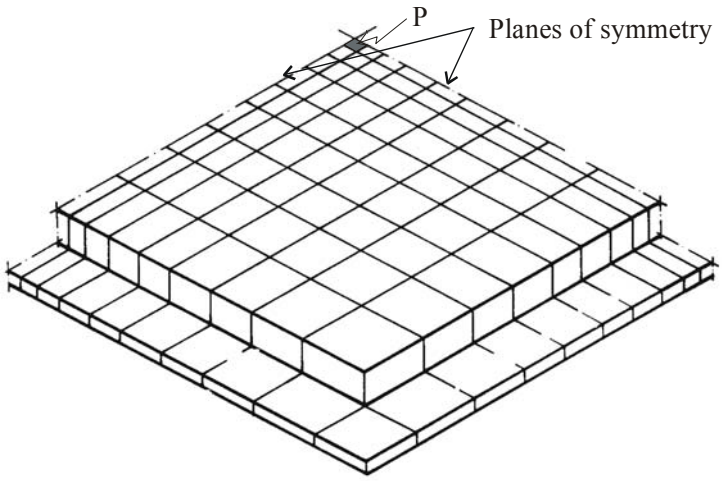

Figure 2-18: The finite element mesh for the model developed by Falkner et al. (1995 b).

The behaviour of the SFRC was modelled by breaking the SFRC into a concrete element and an "equivalent reinforcement" element as shown in Figure 2-19. The concrete element acts in the un-cracked elastic state while the equivalent reinforcement elements acts in the cracked state. The σ-ε response for the concrete element is determined using Young's modulus and the flexural strength. Young's modulus for SFRC is assumed to be the same as that of plain concrete. The flexural strength of the concrete element ($\bar{f}_{ct}$) is calculated to be 15 percent higher than the flexural strength (f_{ct}) estimated from beam bending tests. This is to account for the effect of the post-cracking strength of concrete (represented as a descending dotted curve on the left graph of Figure 2-19). The beam tests were conducted in accordance with the method recommended by the German Concrete Association (1991). During the load increments, after the flexural strength is reached, the concrete element is assumed failed and only the steel fibres are effective and the behaviour is then described by the fictitious reinforcing steel element. The behaviour of the fictitious reinforcing steel element is described by Young's modulus of the steel fibres and a

fictitious yielding strength (f_s) is calculated by multiplying Young's modulus of steel fibre by the cracking strain (ε_R) of the concrete element. Von Mises yield surface is used to describe the biaxial stress state (see the discussion in section 2.3.5.4)

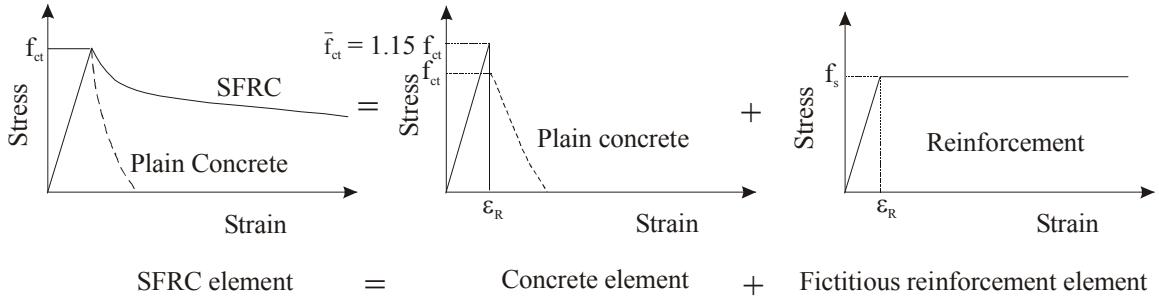

Figure 2-19: The tensile stress-strain behaviour for the SFRC adopted by Falkner et al. (1995 b).

The use of equivalent reinforcement element means that a reinforcing bar that is equivalent to a given steel fibre content is used. The reinforcing action of the steel fibres is assumed to be localised at a depth equal to 55 percent of the thickness of the SFRC slab (Falkner et al., 1995 a). For finite element mesh, the equivalent reinforcement element was overlaid with the plain concrete element. The equivalent reinforcement element will only be active when the plain concrete element cracks.

The assumptions made for the material constitutive relationship are unjustifiable. The material is assumed linear elastic up to a point determined as 1.15 times the flexural strength while the behaviour of an "equivalent reinforcement" is used beyond this point for the cracked SFRC. An unrealistic cracking point is obtained when using flexural strength to characterise the linear-elastic part of the σ-ε response. However, tensile strength (less than flexural strength) should have been used instead which will result in a lower load at the initial crack on the P-Δ response of the slab. In addition, the theory on which the fixed 15 percent extra flexural strength is based is unclear. The amount of this effect will certainly be affected by the concrete strength. The assumption regarding localised reinforcement seems too crude for representing the nature of SFRC as steel fibres are dispersed into the concrete matrix and not localised in a single plane. In this constitutive relation, the post-cracking σ-ε response of SFRC is incorrectly represented by the ductile behaviour of the equivalent reinforcement. The tensile σ-ε response for the SFRC used here (containing 20 kg/m^3 steel fibres) is expected to soften beyond the cracking point rather than behave in a ductile manner (refer to section 2.3.5).

Eight-node brick elements were used to simulate the support layer. The Young's modulus for the cork and the rubber was estimated as 1.4 and 6.6 MPa respectively. The interaction between the slab and the support was simulated using a gap element. The gap element transfers compression

and considers the horizontal friction between the slab and the support. It also allows the SFRC to lift up from the support when tensile forces are generated between the SFRC slab and the support. This idealisation is believed to be more suitable compared to the use of springs, as both the effect of Poisson's ratio and shear stresses can be included in the deformations of the support layer. The gap element is considered to provide an extra advantage to the modelling of ground slabs as it allows the simulation of the horizontal interaction between the slab and the support layer.

Figure 2-20 shows the comparison between the measured and calculated *P-Δ* responses for a SFRC ground slab. The calculated *P-Δ* response is shown to reasonably fit the measured response up to 185 kN. The measured and calculated responses start to diverge significantly at loads beyond 185 kN. The analysis has to some extent provided adequate results with respect to *P-Δ* response for the tested slab. Nevertheless, the stresses and strains obtained during the analysis for the various load increments are incorrect due to misrepresentation of the σ-ε response and due to the used of a single element over the thickness of the slab. This casts doubt on whether this analysis can be extrapolated to analyse ground slabs having different sizes or different material properties.

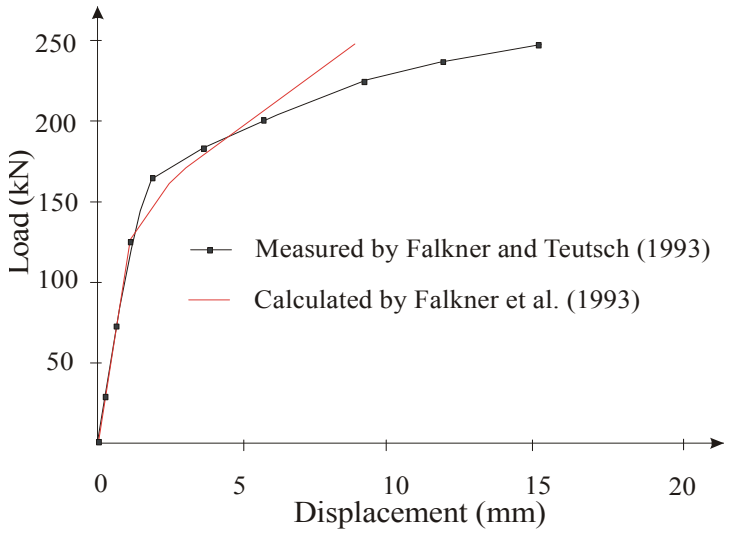

Figure 2-20: Comparison between the measured and the calculated load-displacement responses for SFRC ground slab (Falkner et al. , 1995 b).

2.8.2.2 Finite element model for SFRC ground slab developed by Barros and Figueiras (2001)

Barros and Figueiras (2001) also developed a finite element model to analyse SFRC ground slabs. The experimental results from the full-scale test conducted by Falkner and Teutsch (1993) were used to verify the model (refer to section 2.4.2.1). The finite element mesh for quarter of the SFRC slab is shown in Figure 2-21.

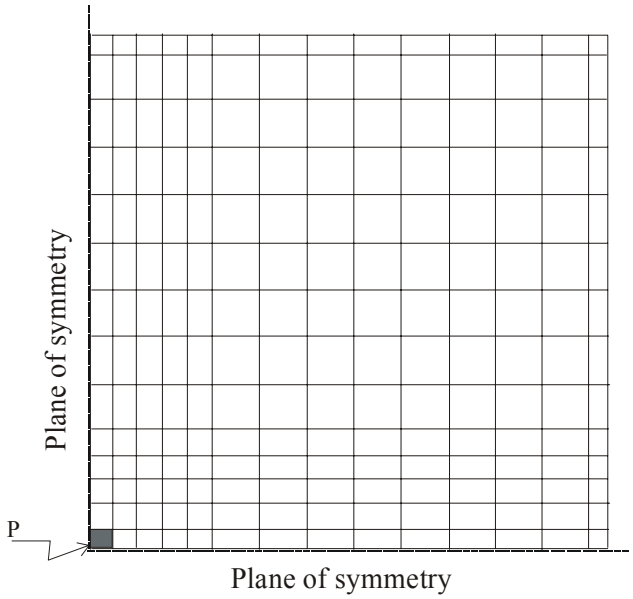

Figure 2-21: The finite element mesh for the model developed by Barros and Figueiras (2001).

Eight-node shell element was used. The thickness of the shell was divided into 10 layers of equal thickness. The use of shell elements is viewed to be suitable for analysing ground slabs. Several layers can be specified over the thickness of the slab and therefore non-linear stress profiles can be captured. The rotational degrees of freedom at shell element nodes should result in improved bending behaviour of the slab compared to the brick elements used by Falkner et al. (1995b).

Cracking of the SFRC was simulated using multiple fixed smeared crack models. The tensile σ-ε response in Figure 2-22 was used in the analysis. Equation 2-26 was used to estimate the fracture energy for the SFRC used in the slab tested:

$$\frac{G_f}{G_{f0}} = 1.0 + 13.159\,(W_f)^{1.827} \qquad (2\text{-}26)$$

where W_f = The steel fibre weight percentage in the mixture.

G_f = The fracture energy for SFRC.

G_{f0} = The fracture energy for plain concrete. It can be estimated from the recommendations given by the RILEM – 50-FMC Committee (1985).

Equation 2-26) was developed by using results from numerical simulation on notched SFRC beams subject to third-point loading. The SFRC for these beams contained 0, 30, 45 and 60 kg/m^3 of hooked-end steel fibres. The compressive strength was between 30 and 60 MPa.

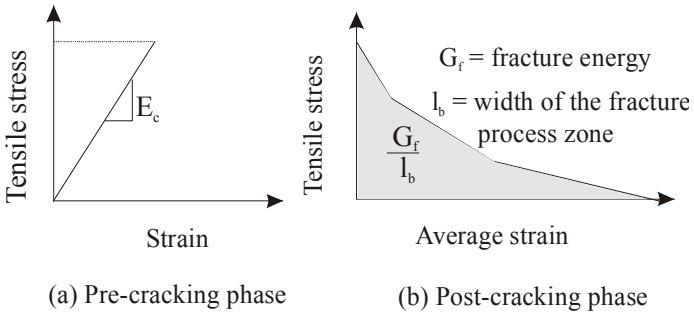

Figure 2-22: The tensile stress-strain response adopted by Barros and Figueiras (2001).

The shape of the softening part of the tensile σ-ε response for the SFRC was obtained from the numerical simulation conducted on notched beams. The width of the fracture process zone (l_b) was assumed to be equal to the square root of the area surrounding the Gauss point. A σ-ε response with exponential softening shape was used to model the compression behaviour of the SFRC.

Non-linear springs were used to simulate the support layer instead of the elastic support assumed by Falkner et al. (1995 b). The non-linear pressure-displacement response was established by performing plate-bearing tests on a 60 mm rubber mat. The plate-bearing test was performed using a 150 mm diameter steel plate. The non-linear response of the tested rubber is shown in Figure 2-23. The springs were set to be orthogonal to the shell elements and applied to all its nodes. The support contribution to the stiffness of the SFRC ground slab (combined structure of the support and the SFRC slab) was calculated by adding the support stiffness matrix to the slab stiffness matrix. At any sampling point where the SFRC slab loses contact with the support, the spring corresponding to this sampling point does not contribute to the stiffness of the SFRC ground slab. It should be noted that the lateral interaction between the slab and the support was neglected.

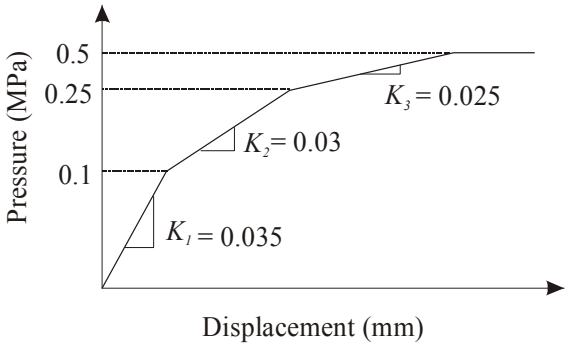

Figure 2-23: Pressure-displacement response for the rubber tested by Barros and Figueiras (2001).

The method used to determine the pressure-displacement relationship for the non-linear springs is sensitive to the size of the loading plate. The standard plate-bearing test is conducted by using a

plate with a diameter of 762 mm and the modulus of subgrade reaction is calculated at a deflection of 1.25 mm (ASTM-D1195, 2004). A smaller diameter plate will yield substantially higher k-values (Bekaert, 2001). Hence, different pressure-displacement relationships can be obtained for the same support layer when using loading plates with various diameters. Therefore, the extrapolation of the test results to establish a single non-linear pressure-displacement response for the support material is doubtful. Nevertheless, the use of a non-linear constitutive material is certainly a step forward towards improved idealisation of the support layers.

Cook et al. (2002) explained the risk involved in simulating foundations by means of discrete springs. This is especially so when higher order elements are used. If a uniform pressure (ρ) is applied downward on the surface of an eight-node element, the resulting nodal forces will be as shown in Figure 2-24. The corner nodes carry upward loads while the mid side nodes carry downward loads. However the sum of all eight nodal loads equals the applied pressure, as must be the case. Therefore, each spring located at an element corner must have negative stiffness. This fits the eight-node element used below the loading plate in the finite element model proposed by Barros and Figuieras (2001). The springs only take compression and thus the corner nodes of this element do not contribute to the stiffness of the SFRC ground slab.

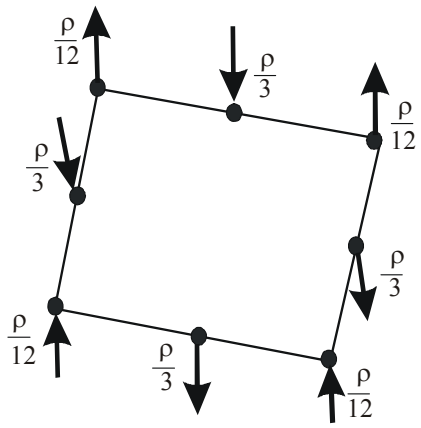

Figure 2-24: Nodal loads related to a downward pressure for eight-node shell element.

Figure 2-25 shows the correlation between the experimental and calculated *P-Δ* responses for a SFRC slab. In spite of the excellent correlation, Barros and Figueiras (2001) recommended that more experiments should be conducted to refine the proposed constitutive laws for SFRC that were utilised in the numerical formulation of the multi-fixed crack model. If the model is extrapolated to analyse ground slabs with different sizes or different material properties, care should be given to the non-linear constitutive relationship for the springs and the use of springs with high order finite elements.

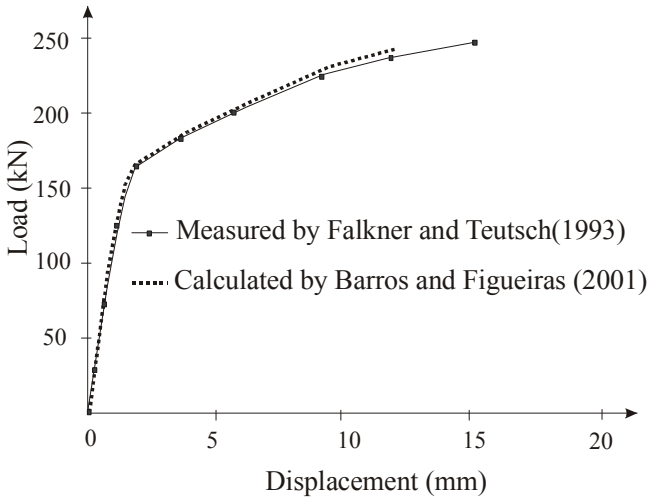

Figure 2-25: Comparison between the measured and the calculated load-displacement responses for SFRC ground slab (Barros and Figuieras, 2001).

2.8.2.3 Finite element model for SFRC ground slab developed by Meda and Plizzari (2004)

Meda and Plizzari (2004) developed a finite element model to analyse SFRC ground slabs. Two SFRC slabs measuring 3000 x 3000 x 150 mm were manufactured and tested. The two slabs contained 30 and 60 kg/m^3 of hooked-end steel fibres respectively. The slabs were loaded in their centres. To reproduce a Winkler foundation, neoprene supports with square base (100 x 100 mm) and thickness of 20 mm were placed under the slabs at 333 mm centres in both directions. The Modulus of the subgrade reaction for the neoprene was determined from plate-bearing test as 0.005 MPa/mm. The finite element mesh for the slab is shown in Figure 2-26. Four-node tetrahedral elements were used. Interface elements were placed at positions along the medians and the diagonals (where cracks are expected to occur).

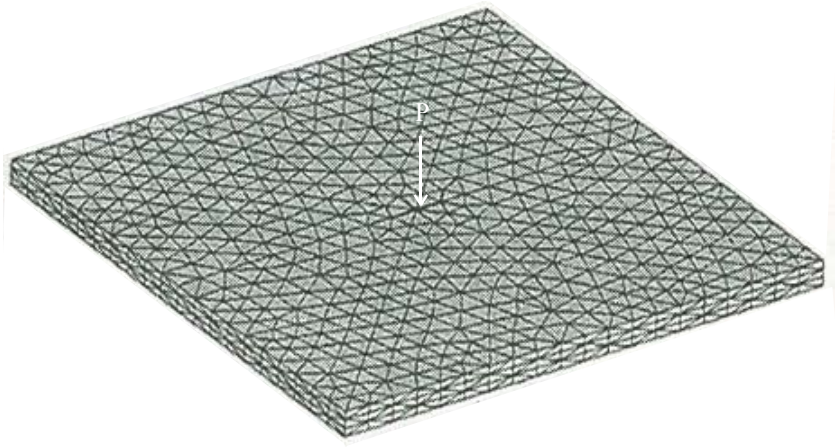

Figure2-26: The finite element mesh for the model developed by Meda and Plizzari (2004).

The cracking of concrete was simulated using the discrete crack approach. The slabs were considered as many elastic sub-domains linked by interface elements that simulate the cracks at pre-defined position. These interface elements initially connect the sub-domains as rigid links and start activating when the tensile stress at the interface reaches the specified cracking tensile strength of the SFRC. As the crack propagates, stresses are transmitted between the crack faces according to the stress-crack opening constitutive relationship. The stress-crack opening relationship was determined by means of finite element simulations of experiments performed on notched beams loaded at third-points. The parameters of the stress-crack opening relationship were determined by means of trail-and-error until best fitting was obtained between the experimental and calculated Load-Crack Mouth Opening Displacement (CMOD) responses. Figures 2-27(a) and (b) show the pre-cracking and the post-cracking responses respectively. The tensile strength was measured from uniaxial tests on cylindrical core specimens.

The neoprene supports were simulated by using truss elements acting vertically and placed at the slab bottom surface and connected to the nodes. The use of truss elements implies that the horizontal interaction between the slab and the support is ignored. Contrary to actual behaviour, tensile stresses are generated in these truss elements when the slab lifts up as they are connected to the slab. As a result, the total stiffness of the slab-support structure (ground slab) will be influenced. In the experimental set-up, isolated neoprene supports are probably used to reduce or eliminate the effect of assumptions usually made when modelling the support of ground slabs. Consequently, the error in the calculated *P-Δ* response due to differences between the actual support layer and the finite element simulation is minimised. The experimental set up is designed to suit the finite element analysis rather than simulating real life ground slabs for which a continuous support layer(s) is usually provided. Therefore, a finite element model that is suitable for the slabs tested here is not necessarily valid for fully supported slabs.

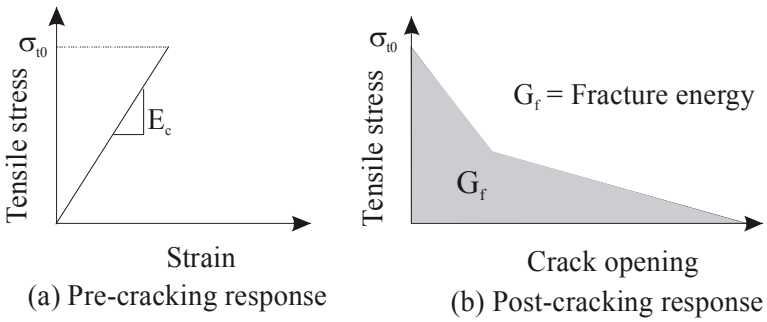

Figure 2-27: The material response adopted by Meda and Plizzari (2004).

Figure 2-28 shows the crack shapes obtained from the experiment and the deformed shape obtained from the analysis of the slabs. The final crack pattern resulting from the finite element analysis was to some extend similar to the results of the experiment. However, the progress of cracking obtained from analysis was found to differ from that observed in the experiment (Meda and Plizzari, 2004).

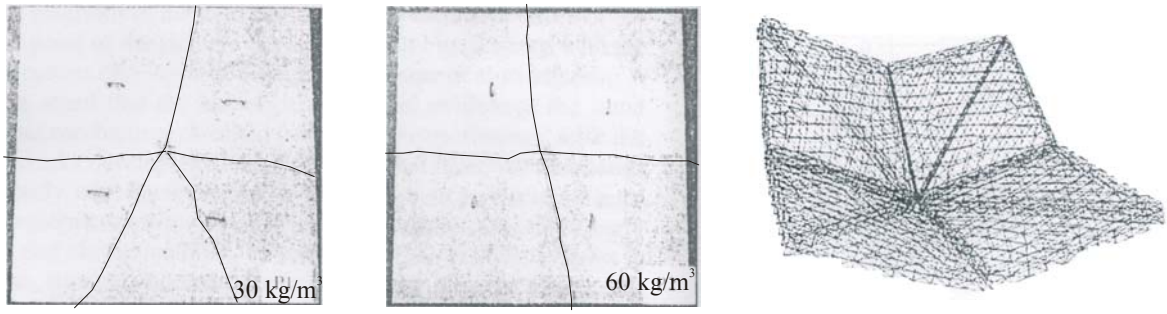

(a) the crack pattern obtained experimentaly (b) the deformed shape

Figure 2-28: Crack patterns and the deformed shape for the SFRC slabs (Meda and Plizzari, 2004).

Figure 2-29 shows the correlation between the measured and the calculated *P-Δ* responses. Based on the presented results, the developed finite element model does not seem to reasonably predict the actual *P-Δ* response. In addition, the analysis is shown to be insensitive to the fibre content. As the differences in calculated *P-Δ* responses for SFRC containing 30 and 60 kg/m^3 are insignificant.

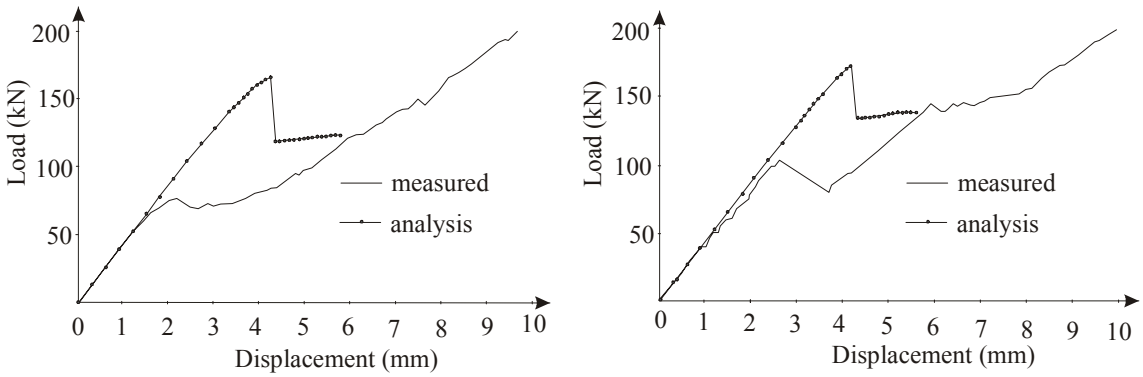

(a) SFRC -30 kg/m^3 (b) SFRC-60 kg/m^3

Figure 2-29: Comparison between the measured and the calculated load-displacement responses for SFRC ground slab (Meda and Plizzari, 2004).

This modelling approach has also been used by Sorelli et al. (2006) to model SFRC ground slabs containing hybrid steel fibres (mixed size steel fibres). In the discrete crack modelling, the interface elements were placed either on the medians or the diagonals instead of placing interface elements at both medians and diagonals. An improved correlation was obtained between the measured and calculated P-Δ responses.

2.9 Summary and remarks

The most significant influence of the addition of steel fibres to concrete has on the composite material is to delay and control the tensile cracking. This improves the mechanical properties of the composite material (SFRC). The post-cracking strength is especially useful in SFRC ground slabs where redistribution of stresses can occur and therefore the load-carrying capacity of the slab can be increased compared to plain concrete. The SFRC slabs were found to provide an equivalent load-carrying capacity compared to conventionally reinforced concrete ground slabs when equivalent percentages of reinforcement is provided.

Existing numerical models used to analyse ground slabs were found inadequate when used for SFRC, as these numerical models do not properly account for the improved mechanical properties of the SFRC. Non-linear finite element analysis can be used to take the post-cracking strength of the SFRC into account thus yielding improved results with respect to actual load-carrying capacity of the slabs. The representation of the cracks and the SFRC constitutive model are the prime parameters affecting the accuracy of the non-linear finite element analysis.

The cracking of concrete has primarily been treated in two different ways. For concrete structures with sufficient reinforcement to assure crack stabilisation, the smeared crack approach is more appropriate than the discrete crack approach. The discrete crack approach is suitable for concrete structures where the number of cracks is limited and the crack path is known. Different formulations are available for the smeared crack approach such as the single-fixed crack, multiple fixed crack and rotating crack formulation. The results of the analysis using these approaches differ, especially beyond the cracking point.

Two approaches exist to model the tensile σ-ε response of the SFRC. In one approach, the law of mixture as well as results from steel fibre pullout tests and results generated from beam direct tension tests have been used. The law of mixture requires that the fibre pullout resistance be mobilised to a large extent when the material reaches its peak stress. This was found not to be the case for the SFRC. The steel fibre pullout tests were found to provide a wide range of results, as the result is mainly dependent on test specimen preparation. Apart from the differences in the steel

fibre parameters, the length of steel fibres inserted into the concrete and the angle at which the steel fibre is inserted into the concrete with respect to the surface of concrete plays a major role in the value of the pullout strength. The direct tension test is cumbersome due to the complexity associated with the gripping of the ends of tested specimen. An alternative approach to model the tensile σ-ε response of the SFRC is to use the fracture energy calculated at specified deflection values on a P-δ response generated by testing SFRC beams. This approach is successful to some extent. Some concerns exist as these methods empirically relate vertical deflections on the P-δ response to horizontal fixed strain values.

Although researchers have agreed on the general shape of the tensile σ-ε response, different methods are used to determine the parameters defining this shape. The testing difficulties and empirical idealisations inherent to existing tensile constitutive relationships are currently hampering the widespread use of SFRC. An appropriate method is needed to determine the parameters of the tensile σ-ε response. One of the aims of this research project will be to develop a method for determining the tensile σ-ε response of SFRC. The resulting constitutive material response is meant to overcome the deficiencies adherent to existing methods. This would eventually enable implementation of SFRC ground slabs designs.

Uniaxial tensile σ-ε responses may be satisfactory to model the tensile behaviour of structural elements that are subjected to biaxial tensile stresses. This is because the controlling biaxial tensile stress is independent of the stress ratio and therefore the strength is almost the same as the uni-axial tensile strength. The addition of steel fibres to concrete has an insignificant effect on the behaviour of the composite subjected to confining pressure and therefore failure surfaces, describing the compression behaviour under multi-axial stress state that were used for plain concrete are also appropriate for SFRC.

Different models have been used for the support layers below the slab. In Winkler's model, the soil was represented in such a manner that the pressure applied over a specific area causes uniform deformation over that specific area but not in the adjacent soil. It allows the modelling of the overall effect of support and does not consider different layers. The use of this model in finite element analysis of ground slabs cause singularities at the bottom of the slab directly under point loads applied at the top. The half-space elastic model defining the Young's modulus and Poisson's ratio was found adequate. The soil is modelled as an equivalent homogenous isotropic elastic layer of uniform thickness, underlain by a rough rigid layer base. This support model allows the modelling of different layers that have different stiffness and it also accounts for shear.

A robust non-linear finite element model is needed to analyse the SFRC ground slabs. The developed model can be utilised to optimise the support stiffness, the steel fibre content and slab thickness for SFRC ground slabs to provide a desired load-carrying capacity. Non-linear finite element analysis of SFRC ground slabs has been conducted previously by other researchers. Several shortcomings and virtues related to these models were pointed out and will serve as base for the finite element analyses conducted in this research. The smeared crack concept will be adopted to represent the cracking of SFRC, as it is more representative to the nature of the SFRC cracking. Lower order shell elements (4-nodes) will be used to analyse the slab as it provides rotational degrees of freedom at nodes which suits the bending behaviour of the slab and it can also be divided into many layers and therefore the non-linear material relationship can be represented through the thickness. Higher order shell elements can also be used based on the adequacy of results obtained from the lower order shell elements. The deficiencies adherent to the use of springs or truss elements to represent the support layers will be overcome by using eight-node brick elements for the support layer. The interaction between the slab and the support will be idealised using an approach similar to that used by Falkner et al. (1995b). Endeavour will be made to investigate the use of a non-linear support material model.